UNIVERSIDADE DE LISBOA
FACULDADE DE CIÊNCIAS
DEPARTAMENTO DE BIOLOGIA

Dissecting how *LAMA2* modulation impact melanoma progression in a 3D *in vitro* model

Érica Sofia Miguel Mocho

Mestrado em Biologia do Organismo e Evolução

Dissertação orientada por:
Prof. Dr. Ana Rita Carlos
Prof. Dr. Rita Zilhão

2025

Acknowledgements

"*Alone we can do so little, together we can do so much*" – Helen Keller

First, I would like to thank my supervisor, Dr. Ana Rita Carlos, for giving me the opportunity to work on this project. Thanks for all your help and support this year. I will always remember to stay positive, even when things are not going so well. I would also like to thank Dr. Rita Zilhão, the project's co-supervisor, for all support, motivation and for being an example and proof that when we truly love something, we can achieve our goals and that knowledge never takes up space.
Next, I would like to express my gratitude to all the members of the EMDD and MMD laboratories, I have learned a lot from you all. Special thanks to Vanessa, who supported me throughout. We achieved incredible things this year, and it would not have been possible without your help and support. I will take with me everything I learned from you, and it goes far beyond laboratory work. I would also like to thank the PhD students Ana, Susana, Diogo and Pedro for sharing their knowledge and always being available to help. They played a key role throughout and provided many enjoyable moments. A huge thank you also to my colleagues, Mariana and Mafalda. This journey would have been much more difficult without you. Thank you for being by my side during the most difficult moments, as well as the good moments. Mariana, thank you for sharing your love of Taylor Swift with me (I'm sure she would be proud of us!) Mafalda, my partner in western blots, thank you for everything, your advice, and the good times (like chasing a giant wasp out of the office!). I would also like to thank Catarina, Fábio and Pedro, you were the first students I had the opportunity to teach and mentor, and this experience helped me to grow too. A special thanks to Joana M. for discussing each result with me and for all the brainstorming sessions. It was a pleasure to work with you. I learn a lot with you, and I hope you continue with your passion about science. Also, a word to Inês C., who engaged the sea urchin world, Gabriela and Solveig, for the discussions in the lab meetings, and Luis M. for always help with microscopy issues. My colleagues Inês G. and Marcelo deserve huge thanks for making the monitoring tasks easier and more enjoyable. It was a pleasure working with you, we were an incredible team. I would also like to take this opportunity to thank Joaquim, Marta, Ana and Rita, who welcomed our group of monitors, guided and teach us. Additionally, I would like to acknowledge the generosity of our donor Henrique Meirelles who chose to support the MATRIHEALTH Project, Fundação para a Ciência e Tecnologia (FCT) (2023.15036.PEX) and the Centre for Ecology, Evolution and Environmental Changes (CE3C) (UID/00329/2025) for funding.
Finally, I would like to express my sincere gratitude to all my friends and family. I would particularly like to thank my friends Carolina, Beatriz S. and Beatriz P., who have been my friends for a long time. Even without realising what I was doing this year, they contributed immensely with happy moments and motivating words. Thank you to my friend Inês F. for all your encouraging words, and for motivating me to broaden my horizons. Thanks also to my friends the 'Evo-Devils', Carolina, André and José, for your support. I am also very happy to have followed your progress and to have seen how much we have all grown and learnt this year. Thank you from the bottom of my heart to my mother for all your love, the wonderful meals that kept me well nourished, your encouraging words and for always providing me with the bases and values necessary to get me to where I am today. To my brother, thank you for being an example of strength and persistence and for encouraging critical thinking. To my sister, I hope to be a good example for you, and I will always be here to advise and support you in all your decisions. Last but not least, a deep and sincere thank you to my boyfriend, Vasco, who supported me through another chapter of my life. Thank you for your constant support and motivation, and for your sense of humour, which so often transformed the most complicated situations.

This past year, I took another important step and achieved another of my goals. I feel that I have grown a lot, and I have been lucky to be surrounded by incredible people along the way. Words cannot express how grateful I am.

Thank you all so much.

Abstract

Melanoma, although not the most prevalent form of skin cancer, is the most aggressive and fatal. Melanoma progression and aggressiveness are dependent not only on the inherent characteristics and behavior of cancer cells, but also on the tumor microenvironment (TME), which surrounds cancer cells and is mainly composed by extracellular matrix (ECM), fibroblasts and immune cells. ECM is a key driver of tumor progression and changes in its compositions and organization can directly influence cancer cell behavior. This project aimed to understand how modifications in ECM components, particularly in the laminin α2-chain (encoded by the *LAMA2* gene) affects melanoma cells, regarding DNA damage, growth, and migration. Melanoma cells (A375 cell line) with *LAMA2* deletion (*LAMA2* KO) were used and DNA damage, growth and their migration capacity, were compared with wild-type (WT) melanoma cells, using both 2D and 3D models (spheroids). Previous data from the host laboratory indicated that A375 *LAMA2* KO cells displayed higher levels of phosphorylated p53. Contrasting, here a decreased in the phosphorylated p53 levels in *LAMA2* KO spheroids with 10 days in culture was observed. Differences were also detected regarding the area of spheroids, with a significant increase in the area of *LAMA2* KO spheroids 20 days after being established. Migration and *RAC1* expression, a regulator of cell migration, were decreased in both 2D and 3D models in *LAMA2* KO cells in comparison to wildtype counterparts. In addition, this project aimed to establish a co-culture system of melanoma and fibroblasts, which was successfully achieved. Collectively, this work advances our understanding of the critical role of the laminin-α2 chain in melanoma and establishes essential assays for characterizing spheroid cultures which more closely mimic the *in vivo* environment. These improved models provide a valuable platform to study tumor biology and microenvironmental interactions with greater physiological relevance.

Keywords: Melanoma, Extracellular matrix, *LAMA2,* Spheroids, Co-culture.

Resumo

O melanoma é um tipo de cancro de pele, que embora não seja o mais comum, quando se apresenta em estádios mais avançados é uma das formas de cancro de pele mais letal. Este tipo de cancro é considerado o 17º mais comum, pela Organização Mundial da Saúde (OMS). O melanoma desenvolve-se a partir da transformação maligna de melanócitos. Os melanócitos são células que produzem pigmento, a melanina, e no caso de estarem localizados na pele transferem a melanina para outras células, os queratinócitos, localizados na epiderme. A melanina tem como principal função absorver a radiação ultravioleta (UV), protegendo assim o núcleo das células. No entanto, a exposição excessiva aos raios solares e consequentemente constantes queimaduras solares, podem causar danos nos melanócitos contribuindo para danos no seu DNA e levar à sua transformação em células cancerígenas (melanoma). Mutações nos genes *BRAF* e *NRAS* são frequentes em nevos melanocíticos (lesões melanocíticas benignas formadas por agregados de melanócitos). A cooperação entre estas mutações e mutações adicionais que possam ocorrer posteriormente, podem tornar nevos melanocíticos em melanoma, conferindo um carácter maligno às células. A progressão das células de melanoma está intimamente associada a modificações do meio onde estão inseridas, também conhecido como o microambiente tumoral. Este microambiente é composto, não só por células cancerígenas, mas também outros tipos celulares como os fibroblastos, células endoteliais e células do sistema imunitário. Outro componente importante do ambiente tumoral é a matriz extracelular (MEC), a qual corresponde a uma rede tridimensional de macromoléculas (principalmente glicoproteínas e polissacarídeos) que ocupa o espaço entre as células dos tecidos, sendo secretada pelas próprias células adjacentes. Estes componentes interagem e influenciam as células cancerígenas, assim como o inverso, em que as células cancerígenas têm a capacidade de recrutar e modelar o comportamento destes elementos conforme as suas necessidades para tornarem o ambiente mais favorável à sua sobrevivência e progressão. Por exemplo, as células de melanoma têm a capacidade de influenciar os fibroblastos, modificando a expressão génica destas células de forma a potenciar progressão tumoral. A MEC é uma estrutura com funções estruturais e funcionais importantes, contribuindo para guiar a morfogénese dos tecidos, assim como crescimento, diferenciação e adesão celular. É composta essencialmente por duas regiões especializadas a matriz intersticial e a membrana basal. A matriz intersticial, a qual permite o preenchimento entre tecidos fornecendo suporte, é composta principalmente por colagénios do tipo I, III e V, e fibronectinas, tendo como principal função mediar processos como diferenciação celular e migração, assim como garantir a integridade dos tecidos. Relativamente à membrana basal, está em contacto direto com as células, e os seus principais componentes são lamininas e colagénio IV que estão envolvidos na sinalização e estrutura, contribuindo para uma função de proteção e de delimitação dos tecidos. As células cancerígenas conseguem remodelar a MEC através de mecanismos como alterações pós traducionais, deposição ou degradação de proteínas da MEC. Estes mecanismos levam a alterações da MEC ao nível da composição, organização das fibras, assim como a sua rigidez (conseguem influenciar de forma a ter um substrato mais rígido ou mais fluído), conferindo um ambiente favorável à sua progressão. As lamininas, localizadas na membrana basal, são glicoproteínas formadas por três cadeias diferentes, uma cadeia α, β, e γ, que organizadas de diferentes formas resultam em diferentes isoformas de lamininas. As lamininas estão envolvidas em diversos mecanismos celulares, entre os quais, adesão celular, migração e proliferação. Devido à sua importante função celular de ancorar as células à MEC, alterações nestas proteínas podem levar a uma perda da ligação entre a MEC e as células, resultando em doenças que afetam principalmente a pele, músculos e nervos. A distrofia muscular congénita relacionada com *LAMA2* (LAMA2-CMD), é um exemplo de doença provocada pela alteração da cadeia α2 das lamininas 211 e 221, devido a mutações do gene *LAMA2.* A alteração da cadeia α2 das lamininas leva a uma disrupção da membrana basal, levando a uma perda de integridade celular. A função de *LAMA2* no contexto do cancro ainda está por explorar, no entanto, vários estudos em diferentes tipos de cancro

demostram que poderá ter um papel importante. Não é possível fazer uma generalização da função de *LAMA2* no cancro, pois os resultados de diversos estudos parecem sugerir que esta função depende do tipo de tumor e até mesmo do estádio. No caso específico do melanoma não há estudos conclusivos relativos à função do gene *LAMA2*, no entanto, é possível que alterações neste gene possam provocar remodelação na MEC e influenciar a progressão e a agressividade do melanoma. Neste projeto o principal objetivo é perceber como é que a deleção do gene *LAMA2* afeta as células de melanoma, relativamente a processos celulares, como danos no DNA, crescimento e migração. Para atingir este objetivo foram utilizadas linhas celulares de melanoma humano (A375), em que se realizou a mutação do gene *LAMA2* (KO), e a mesma linha, mas sem mutação (WT). Foram também utilizados dois modelos diferentes de cultura *in vitro*, o modelo 2D e modelo 3D, servindo também como comparação se o modelo utilizado poderá afetar o comportamento das células e consequentemente levar à obtenção de diferentes resultados. Diversos estudos têm sugerido que há diferenças entre resultados obtidos quando se utilizam modelos 2D ou modelos 3D, e referem que o modelo 3D poderá ser o mais fidedigno no sentido em que as células crescem num contexto mais semelhante ao *in vivo*. Nos modelos 2D as células geralmente aderem diretamente ao plástico, no entanto, em modelos 3D as células estão suspensas, isto leva a alterações da morfologia da célula, sendo que em 3D a morfologia natural das células é preservada. Para além de manter a morfologia celular, os modelos 3D também permitem interações adequadas célula-célula, e célula-MEC, contribuindo para uma melhor mimetização do ambiente *in vivo*. Neste projeto o modelo 3D utilizado foi feito através da formação de esferoides, em que as células estão num poço em suspensão e impedidas de se aderir ao fundo, o que obriga à sua agregação. Como alguns estudos referem que o tempo dos esferoides em cultura pode, também, influenciar o comportamento das células, nomeadamente levar à formação de um centro necrótico devido ao menor acesso a nutrientes e oxigénio, neste projeto analisaram-se esferoides com diferentes tempos de cultura. Foram analisados esferoides com 5, 10, 15 e 20 dias após o dia em que foram plaqueados. Relativamente, ao crescimento, este foi avaliado no modelo 3D, analisando a área dos esferoides ao longo do tempo (medindo o tamanho dos mesmos esferoides ao fim dos dias definidos). Os resultados revelaram que as células *LAMA2* KO apresentam esferoides com áreas maiores do que os WT, ao longo do tempo, possivelmente indicando que existe uma maior proliferação celular ou menor compactação dos esferoides (maior espaçamento entre células). A análise da ativação do p53 em esferoides sugere uma diminuição em esferoides *LAMA2* KO com 10 dias de cultura. No entanto, existem flutuações dos níveis ao longo do tempo, não sendo evidente uma tendência, ou diferenças entre esferoides *LAMA2* KO e WT.

Os resultados obtidos neste projeto, sugerem ainda que o gene *LAMA2* influencia a migração das células de melanoma, tanto no modelo 2D como no modelo 3D. Em particular, observou-se uma diminuição da capacidade de migração nas células de melanoma na ausência de *LAMA2*, comparando com as WT. Foram também analisados genes que estão envolvidos na migração celular. Por exemplo, o gene *RAC1* envolvido na remodelação da actina e promovendo a migração celular foi analisado e verificou-se uma diminuição da sua expressão nas células *LAMA2* KO cultivadas em 2D e em esferoides com 10 dias. Esta diminuição da expressão de *RAC1* vai de encontro ao facto destes esferoides apresentarem uma menor capacidade de migração.

Para explorar como o microambiente tumoral poderia influenciar a progressão das células de melanoma WT e *LAMA2* KO, testaram-se co-culturas em modelo 3D de modo a desenvolver um modelo que replique cada vez melhor o contexto *in vivo*. De forma a ir de encontro a esta vantagem dos modelos 3D, foram produzidos esferoides com células de melanoma e fibroblastos humanas. Desta forma há um aumento da representação do microambiente tumoral, que contribuiu para as respostas sobre o comportamento das células de melanoma. A implementação dos esferoides de co-cultura foi bem-sucedida e a migração foi analisada, comparando esferoides de melanoma WT com fibroblastos e esferoides de melanoma KO com fibroblastos. Não houve diferenças relativas à migração entre os dois

esferoides de co-cultura WT and KO, ao contrário do que acontecia com as monoculturas. No entanto será necessário aumentar o número de experiências para poder ter resultados mais robustos.
Em suma, os resultados desde projeto sugerem que alterações no gene *LAMA2* podem influenciar o comportamento das células de melanoma, podendo mesmo diminuir a sua capacidade de progressão, por exemplo ao diminuir a capacidade de migração destas células, um processo importante para a evolução do cancro.

Palavras-chave: Melanoma, Matriz extracelular, *LAMA2,* Esferoides, Co-cultura.

Contents

List of Tables

List of Figures

List of Abbreviations

2D- Two-dimensional
3D- Three-dimensional
AKT- protein kinase B
AUC- Area Under the Curve
BM-Basement Membrane
BSA- Bovine Serum Albumin
BRAF- B-Raf Proto-Oncogene, Serine/Threonine Kinase
CAF- cancer-associated fibroblasts
cDNA- complementary DNA
CDK2- cyclin-dependent kinase 2
CDKN2A- Cyclin-dependent Kinase-Inhibitor 2A
Ct-Cycle threshold
DSB- double-strand breaks
DMEM- Dulbecco's Modified Eagle's Medium
DNA- deoxyribonucleic acid
ECM- Extracellular Matrix
EMT- Epithelial to Mesenchymal Transition
FAK- Focal Adhesion Kinase
F-actin- filamentous actin
FBS- Fetal Bovine Serum
FFPE- Formalin-Fixed-Paraffin-Embedded
GFP- Green Fluorescent Protein
GFP+- Green Fluorescent Protein Positive
GOI- Gene of Interest
HIF- Hypoxia-inducible factor
HFFF2- Human Foreskin Fibroblasts
HO-1- Heme oxygenase 1
IGF-1- Insulin-like growth factor-1
***LAMA2*-KO**- *LAMA2* knockout
LAMA2-CMD- *LAMA2*-deficient congenital muscular dystrophy
LATS1- large tumor suppression kinase 1
MAF- Melanoma Associated Fibroblast
MAPK-Mitogen- activated Protein Kinase
MITF- Microphthalmia-associated transcription factor
MMP- Metalloproteinase
NER- nucleotide excision repair
NF-kB- nuclear factor kB
NHEJ- nonhomologous end joining
p-p53- phosphorylated p53
PBS- Phosphate Saline Buffer
PFA- Paraformaldehyde
PI3K- phosphoinositide 3-kinase
PiNets- primary intracranial neuroendocrine tumors
PTEN- phosphatase-and-tensin homologue
PVDF- Polyvinylidene fluoride
qPCR- Quantitative Polymerase Chain Reaction
RNA- Ribonucleic acid
ROS- Reactive Oxygen Species
RT- Room Temperature
TBST- Tris Buffered Saline with 0.1% Tween
TGF-β- transforming growth factor-beta
TME- Tumor Microenvironment
TP- Timepoint
TP53- tumor-protein p53
UV- Ultraviolet
WHO- World Health Organization
WT- Wild-Type

1. Introduction

1.1. Melanoma

The term melanoma originates from the Greek words, *melas* (meaning "black") and -*oma* (denoting a tumor) and refers to a type of skin cancer. Based on 2022 data, published by the World Health Organization (WHO), melanoma is the 17th most common type of cancer worldwide, with Europe having the highest incidence (44.1%) followed by Northern America (34%)[1]. Melanoma is consider a rare disease, however it is the most aggressive and fatal form of skin cancer[2]. Melanoma development involves the malignant transformation of melanocytes, a complex process driven by the interaction between genetic and environmental factors, that can result in genetic and/or epigenetic alterations in key genes, controlling proliferation, apoptosis, and response to DNA damage[3,4]. Melanocytes are pigment producing cells of the skin. They originate from a group of highly migratory embryonic cells called the neural crest cells, which during development colonize the skin and numerous other tissues throughout the body[5]. The main function of melanocytes is to produce melanin and transfer it to keratinocytes[6,7], which are located in the epidermis, where melanin exerts its function of protecting the nucleus by absorbing ultraviolet (UV) radiation[4,7]. Sunlight exposure boosts the body's vitamin D production, which is essential for body health. The process requires photolyzing 7-dehydrocholesterol present in epidermis by UVB to previtamin D3 which is then converted to vitamin D3, by thermal isomerization. Then in the liver vitamin D3 is hydroxylated and transported to the kidney where is converted into the biologically active form of vitamin D[8]. Nevertheless, intense UV radiation exposure, without protection, is the major known environmental factor associated with development of melanoma.[4] The excessive sunlight exposure, associated with sunburns can start the transformation of benign melanocytes into a malignant phenotype[4]. Malignant transformation into melanoma follows a sequential genetic model that results in constitutive activation of oncogenic signal transduction. B-Raf Proto-Oncogene, Serine/Threonine Kinase (*BRAF*) and NRAS Proto-Oncogene GTPase (*NRAS)* mutations are frequently found in melanocytic *nevi,* benign skin growths composed of clusters of melanocytes[9]. Therefore mutations in *BRAF* or *NRAS* are not sufficient for a cell to progress into melanoma and this requires the cooperation with other pathways (additional mutations)[10]. For example, mutations in cyclin-dependent kinase-inhibitor 2A (*CDKN2A*) or tumor-protein p53 (*TP53*), which are associated with cell cycle and mutations in phosphatase-and-tensin homologue (*PTEN*), which have implication with immune resistance contributing to tumor progression[3,10]. These *BRAF* and *NRAS* mutations impact additional pathways, as for example the constitutive activation of the mitogen-activated protein kinase (MAPK) signaling and the phosphoinositide 3-kinase (PI3K)/AKT pathway, causing cell growth, proliferation, and cell cycle dysfunction[10]. Once established, melanoma development and progression is essentially composed of two phases: the radial and the vertical growth phase. The radial phase occurs when cancer cells are contained in the epidermis, where tumor growth was initiated, also called melanoma *in situ*. In this phase melanoma cells spread radially through the epidermis. In the vertical phase, cells can spread vertically, and by degrading the extracellular matrix (ECM), invade other tissues turning into metastatic melanoma[11]. The transformation of melanoma *in situ* into metastatic melanoma requires that these cells switch between different phenotypes (have high plasticity)[12]. This phenotypic changes can be a result of an epithelial-mesenchymal transition (EMT), where epithelial cells lose their characteristics, such as polarity, specialized junctions that make them tightly connected, and adhesion molecules (E-cadherin and β-catenin)[13], while acquiring a mesenchymal phenotype that gives a migratory and invasive potential to melanoma cells[11]. EMT is an essential process in embryonic development and cancer progression, since both require similar processes such as cellular invasion and migration to distant sites. During embryogenesis EMT process is responsible for the migration of pre-melanocytes from the neural

crest to the epidermis[11]. While during tumorigenesis, EMT is co-opted as part of the dedifferentiation, a process in which cells lose their specialized features and acquire progenitor-like characteristics[11,14]. In melanoma, dedifferentiation is marked by the reactivation of neural crest-associated genes, and the loss of melanocytic markers[14], and the cells acquire more cellular plasticity enabling this cells to become invasive and initiate tumor metastasis[15]. Cell plasticity is a common characteristic of many cancers, contributing to their heterogeneity, with the coexistence of cells with distinct genotypes, phenotypes and molecular features[16]. The tumor heterogeneity can be distinguished between intratumor heterogeneity, when there is a presence of distinct tumor cell populations within the same tumor, or intertumor heterogeneity that refers to the difference found between tumors of the same type in different patients[17]. In melanoma cells, this plasticity is particularly pronounced, making them one of the most heterogeneous cancers[16]. Melanoma intratumor heterogeneity is largely dependent on the expression of the Microphthalmia-associated transcription factor (*MITF*), the master regulator of melanocyte development, as well as melanoma cell proliferation, survival, and invasion[12,15]. *MITF* levels can influence melanoma shift between two states[15] invasive and non-invasive[15]. Higher levels of *MITF* expression are related with a non-invasive phenotype and a more proliferative state[12]. Proliferative melanoma cells are dependent on high glucose levels that maintain sufficient levels of MITF protein resulting in upregulation of the cell cycle. This occurs through the regulation of different proteins, such as cyclin-dependent kinase 2 (CDK2)[18], essential for G1/S phase transition and DNA synthesis, resulting in increased S-phase populations and robust melanoma cell proliferation[19]. In contrast, glucose restriction decreases *MITF* expression leading to a switch from proliferation to an invasive phenotype, since low *MITF* levels is responsible for upregulation of genes that promote EMT, invasion, and neural crest cell-like properties[12,20]. Additionally, alterations in gene expression can be adaptive responses to cues from the tumor microenvironment (TME), which include not only glucose, but other signals such as hypoxia, amino acid deprivation and ECM mechano-signaling[21]. Melanoma cells interacts with TME through bidirectional communication between melanoma cells and the stroma, via cell-cell or cell-matrix interactions, resulting in TME remodeling, melanoma growth, metastasis and migration[12].

1.2. Tumor microenvironment

Melanoma cells do not exist in isolation. To understand their progression and behavior, it is essential to consider the surrounding environment, also known as TME[22]. TME is a complex and dynamic structure, composed by non-cancer cellular components such as, fibroblasts, endothelial cells and immune cells, that are recruited by cancer cells[22], and the ECM[10] (**Figure 1.1**). The components of the TME affect each other and influence tumor development and progression, impacting cancer cell invasion, tumor growth and metastasis.[23] Importantly, TME composition and behavior can be influenced by factors such as gender, age and lifestyle, turning TME different between patients[24]. Cancer cells are an important regulator of TME, shaping through intrinsic features such as epigenetic alterations, metabolic reprogramming and deregulated signaling pathways[24]. Evidence indicate that epigenetic regulation within cancer cells can drive changes in the TME, for example, the upregulation of a transcription factor, *SNAIL1*, which promotes the induction of the EMT process, by altering the pattern of chromatin modifications[14], facilitating the activation of mesenchymal genes and the repression of epithelial genes[25]. During EMT, the loss of E-cadherin, a cell adhesion molecule, and the increase of N-cadherin, typically expressed in mesenchymal cells, facilitates the escape of malignant melanocytes from keratinocyte control, promoting interactions with stromal cells, such as fibroblasts and endothelial cells[23,26]. At tumor onset, fibroblasts have an anti-tumor role by secreting proteins, such as transforming growth factor-beta (TGF-β), which can act as a tumor suppressor because of its inhibitory effects on the cell cycle[27]. However, tumor cells can escape this inhibitory effect and at later stages, TGF-β acts as a tumor promoter, inducing tumor cell migration pathways[28]. Melanoma cells can also secrete large

amounts of TGF-β, increasing the amount during disease progression[28], thus affecting the microenvironment, promoting tumor growth, and favoring tumor escape to immunosuppressive mechanisms[27]. Fibroblasts, influenced by melanoma cells, change their gene expression, acquiring pro-tumor properties, and differentiate into melanoma-associated fibroblasts (MAFs)[23,28], a subset of cancer-associated fibroblasts (CAFs). MAFs secrete growth factors, such as insulin-like growth factor-1 (IGF-1), which activate MAPK and AKT signaling pathways, increasing cell survival, growth, and migration[23]. Invasion, an important hallmark of cancer, enables cancer cells to acquire a metastatic characteristics. Cancer cell invasion requires both the cell capacity to migrate and the ability to degrade the ECM[29]. Melanoma has the ability to disrupt the ECM using invadopodia, which are actin rich protrusion containing enzymes such as metalloproteinases (MMPs), responsible for mediating ECM degradation[29]. After invading the dermis, melanoma cells change their cytoskeletal organization and communicate with surrounding cells and ECM, enabling them to migrate to distant sites[30]. The ECM facilitates intercellular communication by acting as a storage site for a wide range of molecules, as well as providing a substrate for cell adhesion and migration. Changes in its composition, organization and mechanical properties, such as stiffness directly influences tumor cell behavior[21]. Given the importance of ECM in regulating cell phenotype and behavior, its remodeling is a key driver of tumor progression[24].

1.2.1. The role of extracellular matrix in cancer

The ECM is a dynamic network of proteins with important structural and functional roles in guiding tissue morphogenesis, development and homeostasis though the regulation of cellular physiology, growth, survival, differentiation, and adhesion.[31] The ECM can be divided into two types the interstitial matrix (stroma), and the basement membrane (BM), which differ in composition, function, and location[32] (**Figure 1.1**). The interstitial matrix is mainly composed of collagens I, III, V, fibronectin and elastin, (**Figure 1.1**), and guarantees the structural integrity of tissues, and modulates processes such as cell differentiation and migration. The BM is essential to delimit tissues into different and well-organized compartments, providing structural integrity and barrier protection. The BM is primarily composed of laminins, which allow cells to be anchored to ECM and provide cell signaling cues, and collagen IV (**Figure 1.1**), which is thought to function as the main structural backbone[33]. The ECM interacts with melanoma cells, mainly, through transmembrane receptors such as integrins, that mediated cell-cell and cell intracellular matrix interactions[34]. Integrins also interact with other ECM components, such as laminins and fibronectins, regulating mechanical cues[35] and intracellular signaling pathways, influencing cell behavior by promoting processes such as migration contributing to more invasive and metastatic phenotype[21,32,36]. Cancer cells and tumor-associated stromal cells can remodel ECM by different mechanisms, such as ECM deposition, post translational modifications, and degradation[21], leading to alterations in ECM composition, fiber organization and stiffness, creating a more suitable microenvironment[32]. ECM proteins, such as collagens are synthesized by ribosomes in the rough endoplasmic reticulum where the first post translational modifications take place, and then can be subsequently translocated into the Golgi, where further post translational modifications can occur[21]. One example of these modifications is the crosslinking of collagen which involves the transamination of glutamine residues to the amino group, resulting in formation of covalent bonds that are resistant to proteolytic degradation[32]. This increases stability, and combined with more collagen deposition and linearization of ECM structure facilitating cell migration[21,32]. On the other hand, ECM degradation is primarily driven by MMPs and other proteases, which play a crucial role in melanoma cell motility by cleaving ECM components[32]. These enzymes contribute to the breakdown of the BM, that separates *in situ* melanoma cells from stroma, allowing cancer cells to access the interstitial matrix and invade surrounding tissues. Beyond facilitating invasion, ECM degradation also generates fragments, termed matrikines, which play important roles, including in the activation of signaling pathways involved in

cell adhesion, migration, and proliferation, as well as leading to MMP expression and activation[32,37]. Parallel to ECM degradation, cancer cells can generate forces to open BM pores, if the matrix exhibits mechanical plasticity, creating channels large enough for cells invade through[33,35]. The invasive capacity of cancer cells has been associated with enhanced laminin network rigidity, which might indicate that alterations in these proteins could serve as regulators of tumor cell invasiveness by modifying BM stiffness[38].

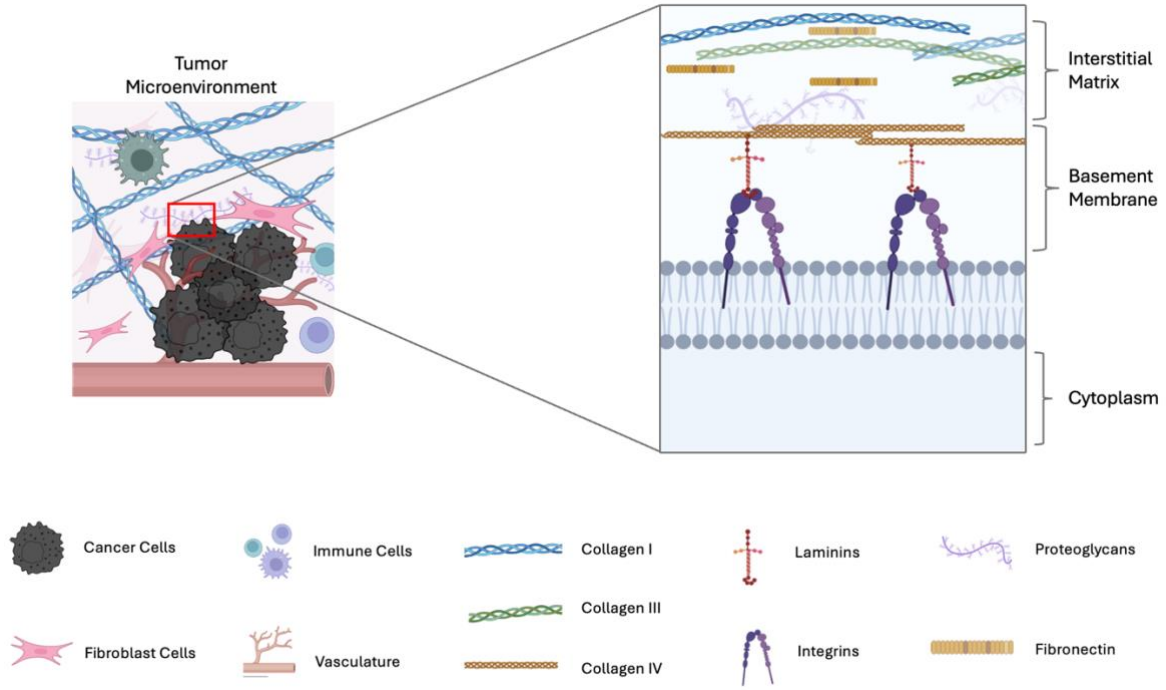

Figure 1.1: Schematic representation of tumor microenvironment (TME) and Extracellular Matrix (ECM). The TME is a dynamic structure surrounding cancer cells and is composed by fibroblasts, immune cells, vasculature, and ECM. These components interact dynamically with the cancer cells, contributing to their growth and progression. The ECM is a key driver of tumor progression and can be divided into two different types: Interstitial Matrix and Basement Membrane (BM). The interstitial matrix is mainly composed of collagens I and III and fibronectin contributing for the structural integrity of tissues. The BM delimitates tissues in well-organized compartments and is mainly composed of laminins and collagens IV. Adapted from Prakash *et al.* 2024[39]. Image created using BioRender.com.

1.2.2. Laminins and *LAMA2* in cancer

Laminins, the most abundant components of the BM, are ubiquitous glycoproteins formed by one α, one β, and one γ chain[31,33]. Five α, four β, and three γ laminin chains can give rise to over 16 different laminin isoforms. Expression of laminin isoforms occurs in a tissue- and cell- specific manner and can vary during development and disease progression[40]. They are strong promoters of cell adhesion, migration, differentiation and proliferation via integrins and other cell receptors including dystroglycan and syndecans[41,42], which recognize laminin isoforms by differentially binding to the laminin chains.[43] Laminins isoforms assemble into polymeric arrays across the cell surface, contributing to the organization of BM with impact on BM integrity and signaling functions. Therefore, changes in this assembly strongly affect cancer cell behavior, by influencing cell function and tissue organization[44]. Many intracellular signaling pathways involved in laminin induced mechanotransduction are initiated at specialized structures called focal adhesions, which link the cytoskeleton to the laminin network[38]. An example is the focal adhesion kinase (FAK), which acts downstream of integrins and play a central role by regulating the localization and activity of various acting-binding proteins involved in filamentous actin (F-actin) remodeling.[38] In addition to modulating actin dynamics, FAK also influences Rho family GTPases, such as RhoA and Rac, which are crucial regulators of cytoskeletal organization, cell adhesion

and cell movement[45] (**Figure 1.2**). For instance, Rac Family Small GTPase 1(*RAC1*) is a gene widely expressed in tissues where it regulates actin cytoskeleton, having an important role in cell migration and invasion[45,46] (**Figure 1.2**). Alterations in laminins and the resulting loss of ECM linkage can lead to various diseases, particularly those affecting the skin, muscle, and nerve[47]. *LAMA2*- congenital muscular dystrophy (LAMA2-CMD) is a disease caused by mutations in *LAMA2* gene. The *LAMA2* gene encodes the α2 chain of laminins 211(LN211) and laminins 221(LN221)[48], which are key structural components in skeletal and cardiac muscle, and in peripheral nervous system[49]. A deficiency or complete absence of laminin-α2 disrupts the BM integrity, leading to mechanical stress[50,51] on muscle fibers, making them more vulnerable to fragmentation resulting in tissue injury and degeneration[49]. In more severe cases, the loss of laminin-α2 is associated with clinical conditions such as hypotonia, skeletal deformity and respiratory insufficiency[49]. The function of *LAMA2* has been well characterized in the context of LAMA2-CMD, however *LAMA2* also appears to play an important role in cancer[42], but its function is not well known and can diverge depending on the type of cancer[42]. The suppression of *LAMA2* in breast cancer could promote the invasiveness of the cancer cells[52]. Nevertheless, depletion of *LAMA2* in bladder cancer cells significantly inhibited their proliferation, weakened invasiveness and migration and promoted apoptosis of these cells[50]. This suggest that alterations in *LAMA2* can have different outcomes depending on the tumor type or stage[50]. In the case of melanoma, the role of *LAMA2* has not been extensively studied. Nevertheless, melanoma cells interact with ECM and laminins, including those containing the α2 subunit, as part of their communication process[53]. Therefore, *LAMA2* alterations could influence the progression and invasiveness of melanoma cells, although further research is needed to clarify its specific effects.

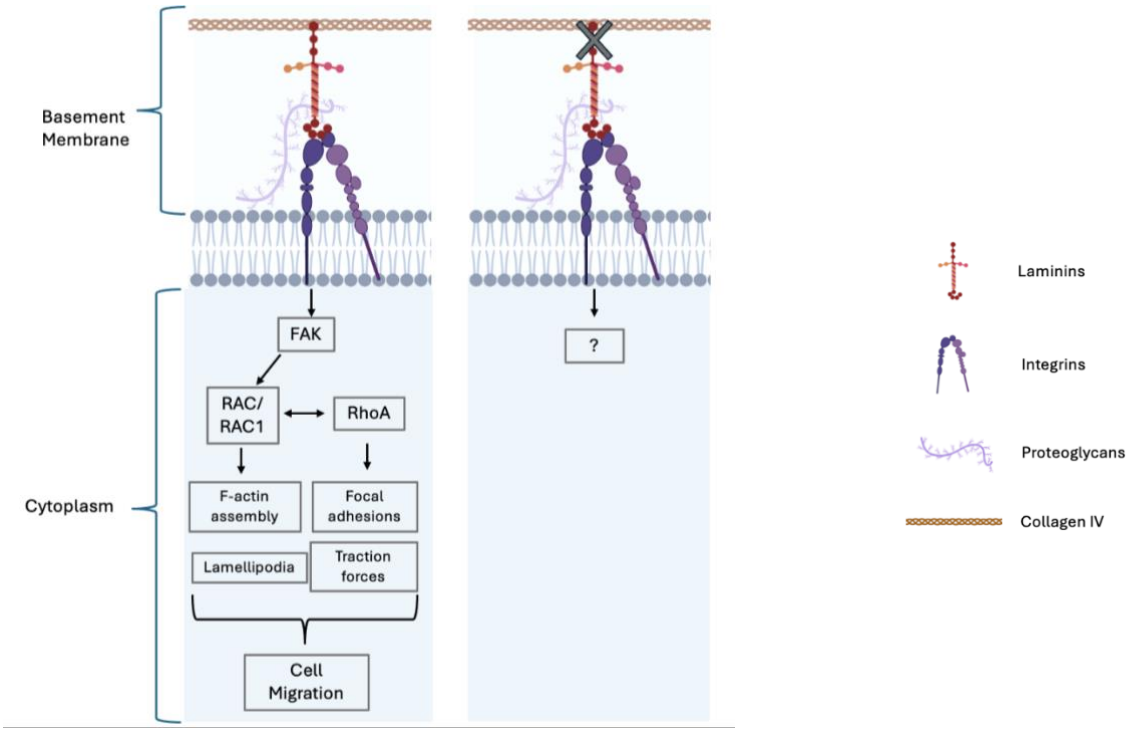

Figure 1.2*:* Illustrative scheme of a pathway induced by laminins to drive cancer cells migration. The signalling pathway involved in laminin induced mechanotransduction are initiated in focal adhesion kinase (FAK), which acts downstream of integrins, and plays a central role by regulating actin dynamics and influences Rho family GTPases, such as RhoA and Rac, which are crucial regulators of cytoskeletal organization, cell adhesion and cell movement. RAC1 is widely expressed in tissue and regulates actin cytoskeleton, having an important role in cell migration and invasion. Adapted from Nonnast *et al*. 2024 [38]. Image created using BioRender.com.

1.3. The role of DNA damage in cancer

The TME and particularly ECM remodeling has been described as key factors contributing to the establishment of the hallmarks of cancer[22]. Besides the contribution to proliferation and metastasis, ECM remodeling has also been implicated in the regulation of the other enabling characteristics of tumorigenesis including oxidative stress and DNA damage[54]. Mutations in genes that encode for important ECM components can contribute to an increase in oxidative stress and DNA damage, as for example observed in the context of *LAMA2*-deficiency, where previous studies showed increased oxidative stress and DNA damage [54,55,56]. On the other hand oxidative stress and DNA damage can also drive ECM alterations by changing the expression of key genes that encode for structural and signaling components of the ECM, including important glycoproteins, such as collagens, fibronectin, and laminins[54]. DNA damage can occur both in ROS-dependent and independent sources, including DNA replication errors, normal cellular metabolism, extracellular sources such as environmental chemicals and sunlight (UV radiation)[57]. Damage in the DNA includes single and double-strand DNA breaks (DSB), base modifications, and crosslinking, all of which contribute to genomic instability, and consequently facilitate transformation and cancer progression[58]. A central player in the cellular response to DNA damage is the tumor suppressor protein p53, often referred to as the "guardian of genome"[59]. Upon DNA damage, p53 can be activated and orchestrates a range of responses. One of these responses is promote DNA repair, activating genes including nucleotide excision repair (*NER*), and nonhomologous end joining (*NHEJ*)[60]. p53 can also prevent cells with damaged DNA from dividing (cell cycle arrest), and in cases of severe DNA damage, p53 can trigger apoptosis, to eliminate cells and prevent potential tumor progression[61,62]. ECM can also influence the DNA damage responses. ECM stiffness, in particular, influences DNA repair capacity[63]. Under low stiffness there is a promotion of apoptosis, by the activation of large tumor suppression kinase 1 (*LATS1*) which links mechanical cues from the microenvironment to the regulation of cell survival[63].

Additionally, several anchorage-dependent cell types such as epithelial and endothelial cells, undergo apoptosis when they do not adhere to the ECM[64]. However, during metastasis, cancer cells lose anchorage dependence and exhibit alterations in their adhesions, which are important for their survival and growth in inappropriate environments[65]. In the context of cancer, it is important to understand whether survival signals from ECM can suppress p53, permitting malignant cell to avoid apoptosis[65]. In most cancers, p53 is frequently mutated, compromising its tumor suppressor activity[61]. Moreover, the loss of p53 was also correlated with an increased of cell motility. ECM proteins that are associated to a migratory phenotype are strongly increased after p53 loss, potentially enhancing cell-ECM interactions to allow cell motility[66]. The p53 loss is related to activation of Rho family of small GTPases, which includes *RAC1*, *cdc42* and *RhoA*, which contribute towards cell migration[66]. In melanoma, the ECM is extensively remodeled, leading to changes in its biochemical and mechanical properties, including stiffness alterations, that can affect the DNA repair mechanisms, by influencing cellular signaling mechanical cues[21,63]. Therefore, understanding how changes in specific ECM components, such laminins, contribute to this remodeling is important to uncover how the TME affects the cellular responses to DNA damage.

1.4. *In vitro* models in cancer studies

As discussed above, cancer and, in this particularly study, melanoma, is a highly complex set of diseases, with dynamic interactions with the surrounding environment. Considering that the ECM plays an active role in tumor progression influencing proliferation, migration, and stress responses, studying these mechanisms requires selecting an appropriate experimental model, including *in vivo, ex vivo* and *in vitro* systems. In this study we used *in vitro* models based on cell lines that have been widely used for research

purposes. They have proved to be useful tools in fundamental studies of cellular pathways and for disclosing critical genes involved in cancer[67]. The use of the appropriate *in vitro* models in cancer research is crucial to investigate genetic, epigenetic, and cellular pathways for the study of proliferation, dysregulation, apoptosis and cancer progression, to define molecular markers and for screening and characterization of cancer therapies[67]. The two-dimensional (2D) culture system has been the most widely used method since the early 1900s. Therefore it has played a vital role in research[68], such as for screening potential treatments and for characterizing proliferation and migration capabilities[69]. However, 2D models also have many limitations as they are inaccurate in representing cells in the *in vivo* context. Cells in 2D are cultured in a monolayer, with more surface area in contact with plastic and culture medium than with other cells[70], forcing them into a polarization that does not reflect physiological conditions[71]. Previous studies showed that cells in 2D respond differently to drugs than cells in three-dimensional (3D) settings[68]. The fact that cells in 2D are forced to adopt an unnatural shape, and since their shape can directly affect their biological activity, may contribute to their different responses[71]. Additionally, and in the context of cancer studies, 2D models are unable to simulate the microenvironment of the original tumors,[72] lacking the structural arrangement of the TME[69], which significantly impacts tumor development[73]. A more realistic *in vitro* model can be provided by 3D cultures[70], as they present some advantages, including the preservation of a closer to natural cell shape, maintaining the cell polarity, and proper cell-cell and cell-ECM interactions contributing to a "niche" more similar to what is present *in vivo*[68]. These characteristics are essential to many functions and steps in cancer, which are important to take in consideration in cancer studies.[71] Spheroids are a type of 3D *in vitro* model, generated from single-cells or with different types of cells cultured together (co-culture)[74], where cells are unable to attach to a surface, forcing their aggregation and consequently spheroid formation[70]. Tumor spheroids have a well-organized heterogeneous architecture containing an outer proliferative layer, an intermediate layer composed of quiescent and senescent cells, and an inner layer, the core, characterized by more apoptotic and even necrotic cells, as a result of the limited distribution of oxygen, nutrients and metabolites in the central part of the spheroids[71,69](**Figure 1.3**). Tumor cells growing as spheroids are able to produce their own ECM[71,73], once again better mimicking the *in vivo* environment. Considering that the TME is characterized by high heterogeneity of cells, 3D models can also allow the co-culture of different cell types, typically stromal cells such as immune cells, or fibroblasts, generating for example multicellular spheroids[74], and recreate a more realistic and diverse microenvironment[71]. Additionally 3D cell culture can also contribute to reduce the need for animal testing, since the results obtained present several similarities with the *in vivo*, and can be cheaper and faster than studies performed in animals [73]. Overall, 3D models appear to be an accurate and valuable tool to explore the role of the ECM in melanoma progression.

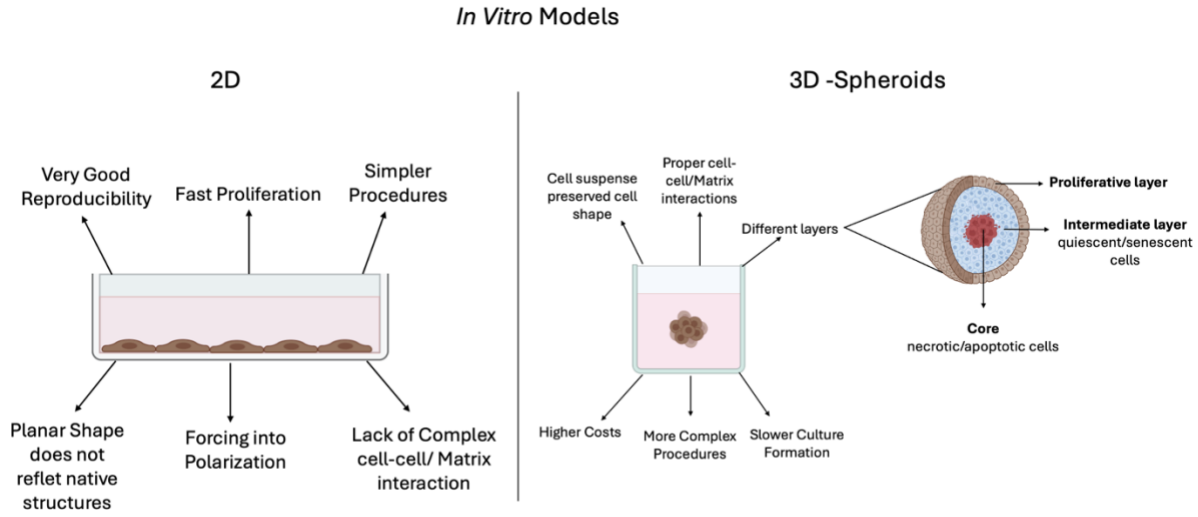

Figure 1.3: Illustrative resume comparing 2D and 3D *in vitro* models. Cells in 2D model are culture in a monolayer, some advantages of this model are the very good reproducibility, and cells have fast proliferation rates. However, there is a lack in cell-cell and cell-matrix interactions. In 3D model, such as spheroids model, cells preserve their cell shape and maintaining polarity. Additionally, spheroids model has a well-organized heterogeneous architecture containing a proliferative layer, an intermediate layer composed of quiescent and senescent cells, and the core, characterized as more apoptotic and necrotic. Adapted from Garnique *et al.* 2024 [75]. Image created using BioRender.com.

1.5. Aim of the project

Alterations in ECM structure can influence tumor onset as well as tumor progression, contributing to the acquisition of a more proliferative or invasive phenotype in case of melanoma. The aim of this project was to understand the impact of laminin-α2 chain-deficiency in melanoma cell behavior. Melanoma cell lines, A375 wildtype (WT) and *LAMA2*-knockout (KO) were compared over time, in terms of cell migration and DNA stability, by using different techniques, including western blot and quantitive PCR (qPCR). This study took into account two different *in vitro* models, 2D and 3D (spheroids). Additionally, with the objective of better mimicing the TME, fibroblasts were co-cultured with melanoma cells. Overall, this project envisaged to provide more insights regarding how ECM alterations can affect melanoma cells and to establish valuable models to characterize melanoma progression.

2. Material and Methods

2.1. Cell Culture

A375 human melanoma WT and KO cells lines and human foreskin fibroblasts (HFFF2) were cultured in Dulbecco's Modified Eagle's Medium (DMEM) supplemented with 10% of fetal bovine serum (FBS) and 1% of an antibiotic mixture: penicillin (10,000 U/mL) and streptomycin (10 mg/mL), and incubated at 37ºC, 5% CO_2 with constant humidity. When confluency reached approximately 70%, cells were passaged, using Trypsin-EDTA. KO cells lines were previously generated[76] and two independent single cell clone were used in the current study.

2.2. Spheroid Formation

2.2.1. Monoculture Spheroids

Spheroids were generated using A375 cell lines (WT or KO) or HFFF2 cells. First the cells were counted to obtain a concentration of $5x10^5$ cells/mL and 20 µL of cells suspension were plated in a 96-well plate, previously coated with 1% of agarose in 1x PBS (phosphate buffer saline) to prevent cell adhesion, and filled with DMEM complete medium. To potentiate the aggregation, the 96-well plates were placed in a shaker with circular motion, for 10 minutes at 70 rpm. The spheroids were kept in the incubator at 37ºC and 5% CO_2 with constant humidity.

2.2.2. Co-culture Spheroids

Co-culture spheroids were generated using A375 (WT or KO) cell lines and HFFF2 GFP+ cells. First, 20 µL of a 10 000 cells/mL suspension of $HFFF2^{GFP+}$ cells were plated in 96- well plates and were placed in a shaker with circular motion, for 10 minutes at 70 rpm. $HFFF2^{GFP+}$ spheroids grew for 3 days. After this period 20 µL of a 2500 cells/mL suspension of A375 cells were added to the $HFFF2^{GFP+}$ spheroids and were placed in a shaker again. The spheroids were kept in the incubator at 37ºC and 5% CO_2 with constant humidity.

2.3. Spheroids Area Measurement

For each condition, four spheroids were observed under a brightfield microscope Olympus CK2 and images were acquired. The area was measured using ImageJ.

2.4. Migration Assay

2.4.1. Migration Assay in 3D spheroid model

Six spheroids from each cell line and each time point were transferred, using a cut micropipette tip, into a 96-well plate previous coated with 0.1% of gelatin for 2h and blocked with 1% bovine serum albumin (BSA) for 1 hour, and filled with 200 µL of DMEM supplemented with 2% of FBS and 1% of an antibiotic mixture: penicillin (10,000 U/mL) and streptomycin (10 mg/mL). After transfering the spheroids, images of each spheroid were acquired at 0h (60 minutes after transfer), 6h, 24h, and 72h (**Figure 2.1**), using an Olympus CK2 microscope.

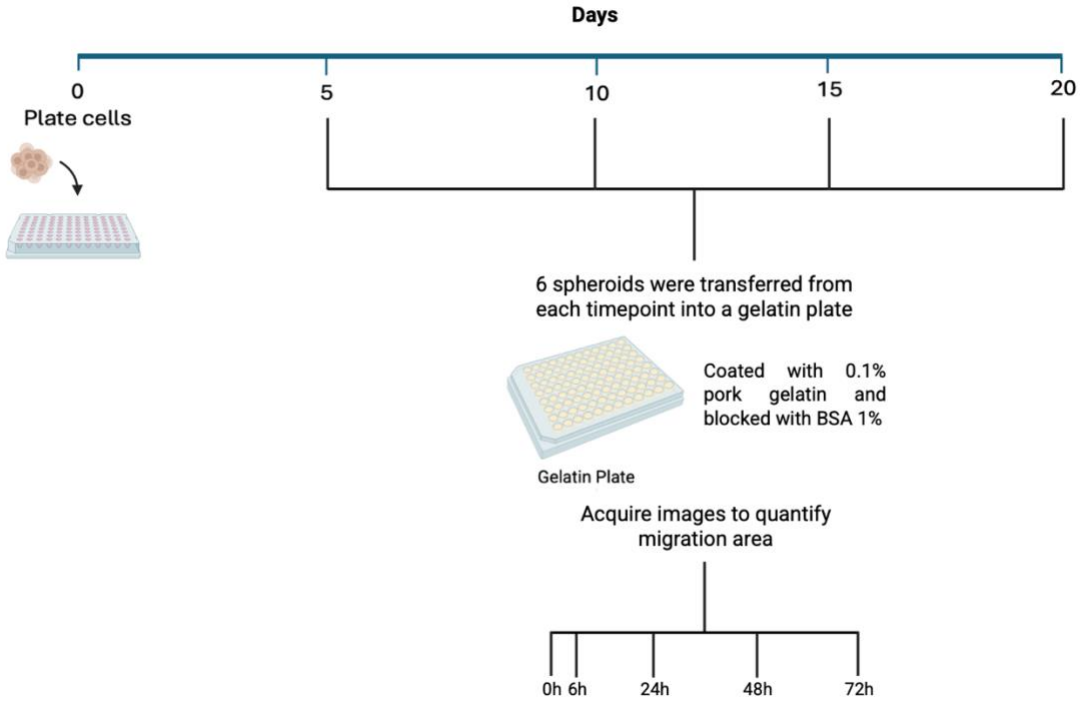

Figure 2.1: Illustrative scheme of migration assay. A375 WT and *LAMA2*-KO spheroids were plated and after 5, 10, 15, and 20 days post seeding six spheroids from each timepoint were transferred into a 96-well plate. The migration plate was previously coated with 0.1% gelatin and blocked with 1% BSA in 1x PBS. To analyze migration, pictures were acquired at 0, 6, 24, 48, and 72h after being transferred to the migration plate and the migration area was quantified. This scheme was created using Biorender.com.

The area was measured using ImageJ. The calculation of the migration area was done by calculating the difference between the core of the spheroids and the total area and normalize for the 0h. The protocol was adapted from literature[77].

2.4.2. Migration Assay in 2D model

A375 WT and KO cell lines were plated in 6-well plates and, when they reached 90-100% confluency, four scratches with a micropipette tip were made to promote cells migration. The wells were washed with 1x PBS and 2 mL of DMEM, supplement with 0.1% of FBS and 1% of an antibiotic mixture: penicillin (10,000 U/mL) and streptomycin (10 mg/mL) were added to each well. After 72h cells were collected into eppendorf tubes. Then the pellet was centrifuged at 500g during 5 min, the supernatant was removed, and the pellet was washed with 500 µL 1x PBS and centrifuged again. The 1x PBS was removed and the pellets were stored at -20ºC, to further extract RNA.

2.5. Western Blot

2.5.1. Protein Extraction

Spheroids were collected into eppendorf tubes, centrifuged and washed with 1x PBS. After they were suspended in 75 µL of SDS-PAGE (20% Glycerol, 4% SDS 100mM, Tris pH 6.8, 0.2% Bromophenol blue, and 100mM DTT). They were then homogenized using a Retsch MM400 Tissue Lyser to shred the cell membrane. The obtained lysate was heated at 50ºC for 10 minutes and then centrifuged at 4ºC and maximum speed for 5 minutes. The supernatant was transferred to a new microcentrifuge tube and

protein concentration was determined by the ratio of 260 nm to 280 nm absorbance using a NanoDrop One. Samples were stored at -20ºC until use.

2.5.2. Western Blot

Proteins were separated using a 10% polyacrylamide gel. Protein extracted from spheroids samples was loaded in the gel (approximately 75-100µg of protein per well) and then run in 1x running buffer (3.02g Tris base, 14.42g Glycine, 1g SDS in 1L distilled water) at 150 V for 1h, using the Mini-PROTEAN Tetra electrophoresis system (Bio-Rad). Next, proteins were transferred to a polyvinylidene fluoride (PVDF) membrane previously activated with methanol. The Mini Trans-Blot Cell (Bio-Rad) was then used for protein transfer with chilled transfer buffer (5.82g Tris, 2.93g glycine in 1L distilled water) at 100 V for 45 min. After transfer, to confirm the quality of protein extracts and verify the loading of the gel, GelCodeTM Blue Safe Protein Stain (ThermoFisher Scientific) was used to stain the gel. Membranes were next blocked for 1h in 5% milk in TBST (20 mM Tris, 150 mM NaCl, 0.1% Tween20 and distilled water (dH_2O), pH 7.4-7.6), with agitation. Membranes were rinsed 3 times in TBST and incubated with the primary antibody, diluted in 2% or 5% BSA in TBST and 0.02% Sodium Azide overnight at 4ºC, with agitation. After, membranes were washed with TBST and then incubated with secondary antibodies diluted in 5% powdered milk in TBST for 1h at RT. After the incubation with the secondary antibody, membranes were washed 3 times, for 10 min each, in TBST and chemiluminescence was detected using SupersignalTM West Pico Chemiluminescent Substrate HRP (ThermoFisher Scientific). Images were acquired using Amersham Imager 680 RGB (GE Healthcare) and the densitometry analysis was performed using ImageJ. Antibodies used are listed in **Supplementary Table 1**.

2.6. Formalin-Fixed Paraffin-Embedded (FFPE) Spheroids

To detect the presence of proteins of interest in spheroids by immunofluorescence, spheroids were plated in low attachment 96-well plates, filled with 100 µL of DMEM. A drop of 20 µL of A375 WT and *LAMA2* KO cell lines suspension in a concentration of $5x10^5$ cells/mL were added to each well. Then the plate was placed in shaker for 10 min at 70 rpm. Spheroids were maintained for 5, 10, 15, and 20 days in the incubator at 37ºC and 5% CO_2 with constant humidity. When spheroids reach the target day (5, 10, 15, or 20 days post seeding) the DMEM was totally removed carefully to not disaggregate the spheroid and 50 µL of HistoGel™ was added to fix the spheroids. After HistoGel™ solidified (with cold exposure) the spheroids were removed from the plate, placed into cassettes, and fixed with 10% buffered formaldehyde for 8-12 hours. After, the spheroids were prepared for paraffin embedding by series of alcohols increasing concentration and xylene immersions. Later, the spheroids were sectioned using a microtome, cutting 4 µm-tick sections. Sections were mounted onto TOMO adhesive slides and placed in an oven for 1 hour at 60ºC to ensure proper adhesion to the slide.

2.6.1. Immunofluorescence

Slides with FFPE spheroids sections were deparaffinized using xylol for 10 minutes. Then the slides were washed with distilled water. After removing all the paraffin from the slides, a heat retrieval treatment was performed, using citrate buffer. The slides in 1x citrate buffer were heated in the microwave during 2 minutes at 750W and when the liquid started to boil, the potency was decreased to 150W for 4 more minutes. The slides were left to cool down at room temperature. After the slides were placed in Tris- Buffered Saline with Tween 20 (TBST). Using a PAP pen, a circle was drawn around the section of interest (section that contains the spheroids), to avoid the mixing of the applied antibodies.

For permeabilization the spheroids were covered with 0.3% Triton in 1x PBS and incubated for 15 minutes. Then the spheroids were incubated with goat serum diluted in TBST (1:50) for 60 minutes. After blocking, the spheroids were incubated with the primary antibody (**Supplementary Table 1**), overnight at 4ºC in a dark and wet chamber. Next day, the spheroids were washed in TBST and incubated with secondary antibody during 2 hours at room temperature, in a dark and wet chamber. After incubation the spheroids were washed with 1x PBS. Spheroids were mounted using Mowiol-DABCO (2.4g of Mowiol, 4.8 mL of 100% glycerol and 2.5% DABCO in H2O; pH 8.5) with DAPI (25µg/mL). The immunofluorescence images were acquire using an Olympus BX60 microscope and analyzed using ImageJ.

2.7. RNA extraction and qPCR analysis

Spheroids from migration assays were collected and placed in eppendorf tubes, centrifuged and washed with 1x PBS. After, the pellet was lysed with 500 µL TRIzol™ reagent and homogenized using Tissue Lyser for a mechanical disruption, during 30 Hz for 2x2 minutes. To completely dissociate the nucleoproteins complex, samples were incubated for 5 minutes in TRIzol™ reagent and then 100 µL of chloroform was added to the tube vortexed and incubated for 3 minutes. After incubation, samples were centrifuged for 15 minutes at 12 000g at 4ºC allowing the separation of the solution in different phases. A lower red phenol-chloroform phase, an interphase, and a colorless upper aqueous phase (phase of interest that contains RNA). The phase with RNA was carefully transferred into a new tube, to avoid contamination with other phases. To isolate RNA, 250 µL of isopropanol was added and incubated for 10 minutes followed by 10 minutes of centrifugation at 12 000g at 4ºC. The precipitated RNA forms a white gel-like pellet, and the supernatant was discarded. The pellet was resuspended in 500 µL of 75% ethanol and tubes were vortex and centrifuged for 5 minutes at 7500 g at 4ºC. After centrifugation the supernatant was discarded and the pellet was again resuspended in 75% ethanol, vortexed and centrifugated again. The obtained supernatant was removed and the pellet was air dried. After, the pellet was resuspended in 20 µL of RNase-free water and incubated during 10 minutes in a thermoblock at 55ºC. Using Nanodrop, the concentration of RNA was quantified, and the RNA was store at -20ºC. Using previously extracted RNA, complementary DNA (cDNA) was synthetized using Xpert cDNA synthesis Kit (#GK86.0100). In an RNase-free microtube the following components were added to 1 µg of template RNA, 3 µL of the Xpert cDNA Synthesis Supermix (5x), and RNase-free water to complete the volume up to 20 µL. The tubes were gently mixed, briefly centrifuged and placed in a thermocycler at 37ºC for 15 minutes and then at 60ºC for 30 minutes. The enzyme RNase was inactivated by heating for 3 minutes at 95ºC and then was stored at 20ºC until being used for quantitative PCR (qPCR).
For qPCR, a reaction mix were prepared using 5 µL of Xpert Fast SYBR 0.4 µL of reverse and 0.4 µL of forward primer (**Supplementary Table 2**) and 3.2 µL of RNase-free water, making a total of 10 µL total volume. The mixture was distributed in 96-well plates and 1 µL of cDNA were added to each well. To do replicates, each sample were run in duplicated. The plate was sealed with an optically transparent film and centrifuged, and the qPCR reaction was performed in a CFX96TM Real-Time PCR Detection System (Bio-Rad). After checking the quality of the qPCR reactions by melting curve analysis, the threshold cycle (Ct) values of the gene of interest (GOI) and the housekeeping gene were compared, according to the following equations **2.1** and **2.2** to analyze qPCR reaction:

$$DCt = Ct_{GOI} - Ct_{Housekeeping} \quad \textbf{(2.1)}$$

$$\text{Fold difference to housekeeping} = 2^{-DCt} \quad \textbf{(2.2)}$$

2.8. Metaphase spreads and analysis of chromosome aberrations

A375 WT and KO cells were plated ($7x10^5$ cell per 10 cm dish) and, on the following day, colcemid (0.1 mg/mL final concentration) was added to the growth medium for 4 hours. The growth medium containing cells in metaphase was collected and then cells remaining in the dish were washed with 1x PBS to collect the remaining cells in metaphase. After centrifuging, pre-warmed (37 ºC) hypotonic buffer (0.075M KCl) was added, drop by drop, onto the cells, which were then incubated at 37 ºC for 25 minutes to swell the cells and separated the chromosomes. After incubation, 3 drops of fresh ice-cold fixative (methanol: acetic acid, 3:1) were added to prepare cells for staining and preserving cellular structure and were centrifuged for 10 minutes at 600 g. DMEM was aspirated leaving 1 mL, to which 2 ml of ice-cold fixative were added dropwise while vortexing and then, 9 mL were additionally added. Cells were centrifuged again, and the supernatant was removed. The pellet was resuspended in 250 µL of fixative and placed at -20 ºC for 15 minutes or for long term storage. To spread metaphases, first the slides were placed in a coplin jar with methanol and wiped with cotton tissue. Next, 45% of acetic acid was added to the slides, the excess was removed, and cells were immediately dropped (each drop was 20 µL). After slides were dried, they were stained with Giemsa for 5 minutes. Slides were rinsed with distilled water three times and left to dry. Slides were then observed under a brightfield Olympus BX51 microscope and images acquired with a DFK 23U274 camera. Images with metaphases were analyzed for the type of chromosomal aberration, including fusions, gaps, breaks or radial chromosomes, and the number of these aberrations per metaphase was analyzed and counted using ImageJ.

2.9. Statistical Analysis

Statistical analysis of the results was performed using the GraphPad Prism 8.0.2 software. A one-way ANOVA with Dunnett's multiple comparisons test was used for p-p53 analysis, for each timepoint, migration and gene expression between WT and KO in 2D and 3D migration. A two-away ANOVA with Dunnett's multiple comparisons was used for the area analysis.

3. Results

3.1. Effect of *LAMA2*-deficiency on DNA damage in melanoma cells

Previous results from the host laboratory showed that *LAMA2* KO (KO) melanoma cells tend to display higher levels of DNA damage and increased p53[76,78]. To further support this data, chromosome aberration of WT and KO cells were analyzed. For KO cells, two independent single cell clones were used to confirm that the results observed were not unique to a single clone. Chromosomes in metaphase were stained with Giemsa (**Figure 3.1A**) and then analyzed by counting the number of aberrations *per* metaphase (**Figure 3.1B**). The results showed a mild tendency towards an increase of aberrations in melanoma KO cell lines. However, more samples are needed to confirm this result.

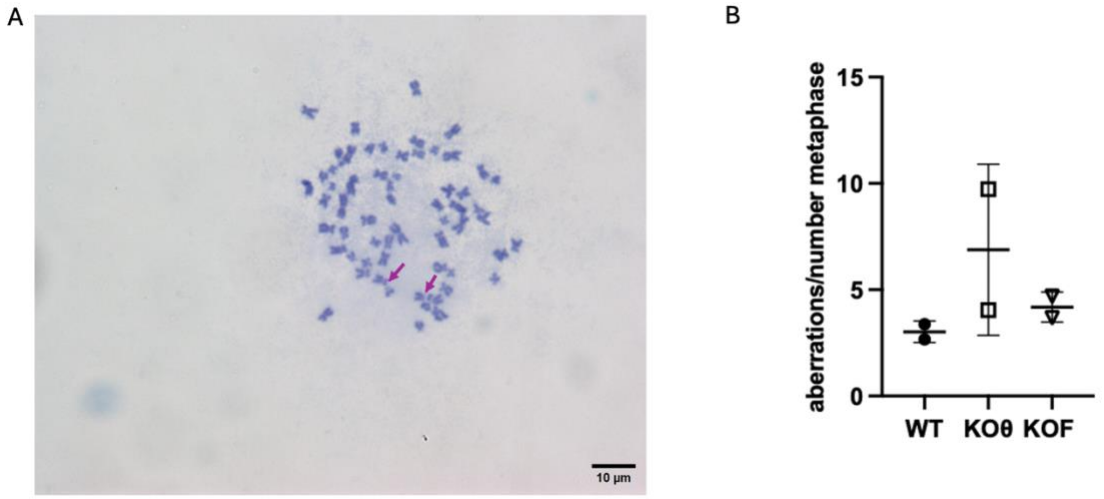

Figure 3.1: *LAMA2*-deficiency may cause a mild chromosome aberrations in melanoma cells. A375 wildtype (WT) and *LAMA2*-KO (KO) cells, using two different single cell clones, treated with colcemid were stained with Giemsa and chromosomes were observed. **(A)** Representative image of a metaphase. Pink arrows indicate examples of aberrations that were identified. **(B)** The total number of metaphases and the number of aberrations (break, fusions and GAPs) per metaphase was analyzed. N=2 independent experiments.

In addition, to understand if the increased of DNA damage previously observed[78], and the tendency observed in this study for chromosome aberration, was also present when using a 3D spheroid model, DNA damage was analyzed at day 5 of spheroid formation and revealed an increased in KO spheroids when compared to the WT ones (Vanessa Ribeiro, unpublished).

To analyze the DNA damage over time in 3D cultures, the levels of phosphorylated p53 (p-p53) were also analyzed in WT and KO spheroids across different time points (5, 10, 15 and 20 days) (**Figure 3.2A**). Data was normalized to WT melanoma spheroids with 5 days to understand if p-p53 protein levels change over the time. The results obtained did not show an evident tendency of the p-p53 levels over time (**Figure 3.2B)**, and the levels of p-p53 between replicates for each timepoint have some variation which makes it difficult to conclude whether there is a difference between the WT and KO spheroids.

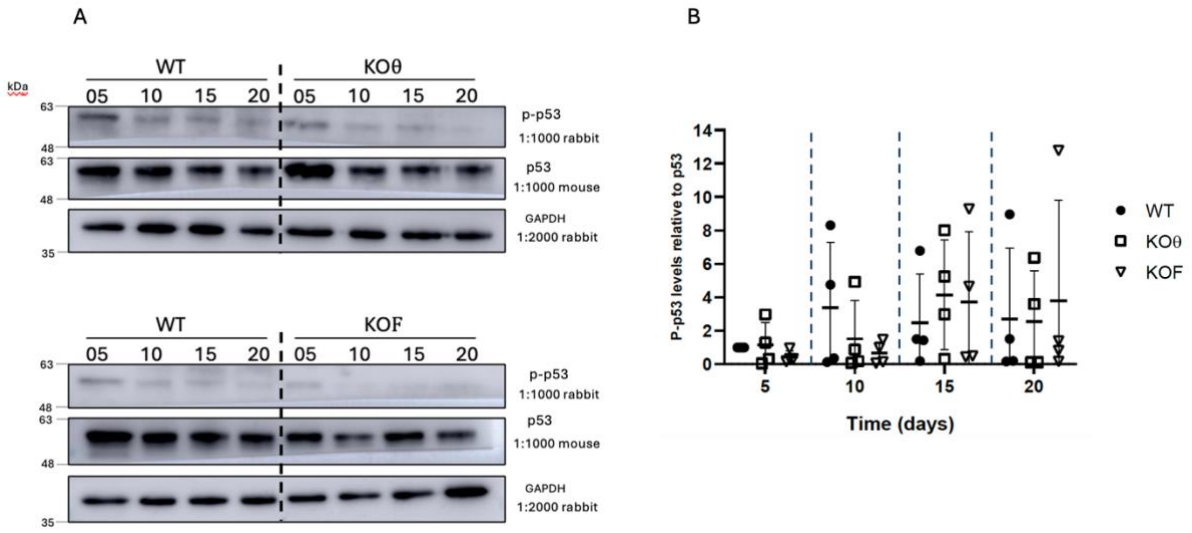

Figure 3.2: Evaluation of p-p53 levels in melanoma spheroids during time. A) A375 WT and KO cells were plated in a 96-well plate coated with 1% agarose in 1x PBS, at a concentration $5x10^5$ cells/mL. Two independent *LAMA2*-KO single clones were used KOθ and KOF. A drop of 20 µL were added to the well previously filled with 100 µL of DMEM. After, the plate was shacked in circular motion to promote aggregation, during 10 minutes at 70 rpm. A375 WT and LAMA2-KO spheroids (with 5, 10, 15 or 20 days) were collected and protein was extracted to analyze the phosphorylation of p53 at serine 15 (p-p53) by western blot. p53 was used as control for p-p53 and GAPDH was used as a loading control. For p-p53 a rabbit secondary antibody was used, and for p53 a mouse secondary antibody, both in a concentration of 1:1000. For GAPDH a rabbit secondary antibody was used with a concentration of 1:2000. **B)** Quantification of the p-p53, using ImageJ and results were normalized for WT with 5 days. N=4 independent experiments.

The data displayed in Figure 3.2 were reanalyzed and individual plots were generated for each timepoint (5, 10, 15, and 20 days) (**Figure 3.3**), in order to enquire if there was a difference between the WT and KO melanoma spheroids at any given timepoint. Taking into account the variability between experiments, the results were normalized to the WT for the correspondent timepoint (**Figure 3.3**).

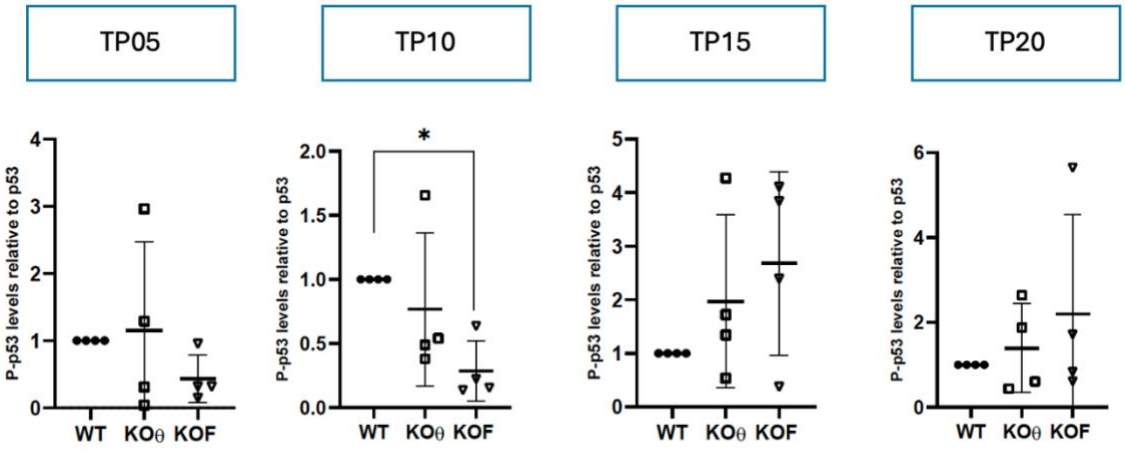

Figure 3.3:The absence of *LAMA2* impacts the levels of p-p53 in 10-days melanoma spheroids. A375 WT and KO cells were plated in a 96-well plate coated with 1% agarose in 1x PBS, at a concentration $5x10^5$ cells/mL. Two independent *LAMA2*-KO single clones were used KOθ and KOF. A drop of 20 µL were added to the well previously filled with 100 µL of DMEM. A375 WT and LAMA2-KO spheroids (with 5, 10, 15, and 20 days) were collected and protein was extracted to analyzed phosphorylation of p53 at serine 15 (p-p53) by western blot. p53 was used as control for the p-p53. GAPDH was used as a loading control. Quantification of the p-p53, using ImageJ and results from each timepoint were normalized for WT. N=4 experiments. Statistical analysis was performed by a One-Way ANOVA with Dunnett's multiple comparisons. *=$p<0.05$.

In spheroids cultured for 5 days (TP05) the results showed a tendency for a decreased in p-p53 levels between the WT and KOF spheroids. This tendency became significant in spheroids cultured for 10 days (TP10), the KOF spheroids showed a decrease of p-p53 levels comparing with the WT. Additionally,

even though not significant, KOθ also showed a tendency towards a decreased. For spheroids cultured for 15 days (TP15), the tendency was inverse and KO spheroids tend to have an increase in p-p53 levels compared to WT. Regarding the last timepoint (TP20), spheroids cultured for 20 days, the tendency is lost and there are no differences between the WT and KO spheroids. The results suggest that *LAMA2* -deficiency tends to reduce DNA damage in melanoma spheroids, in contrast with 2D models where *LAMA2* KO tend to show increased DNA damage.

3.2. Absence of *LAMA2* increases the area of the melanoma spheroids

Since p53 can impact cell proliferation[59], and changes in proliferation can affect spheroid formation and maintenance, it is important to analyze the area of the spheroids to see what happens over time and the assess any differences between the WT and KO spheroids. To achieve this goal WT and *LAMA2*-KO spheroids were generated, and their area was analyzed by measuring the total area of the spheroids on days 5, 10, 15, and 20 post seeding (**Figure 3.4A**). The results were then analyzed using ImageJ, by drawing a segmented line and measuring the total area of the segment **(Supplementary Figure 1**). The results showed a significant increase in the area of KOs spheroids, compared to the WT in each timepoint (**Figure 3.4B**). Additionally, the two single cell KO clones (KOθ and KOF) showed similar results in each timepoint. This analysis indicates that WT and KO spheroids area is different, and this difference started in an early timepoint (spheroids cultured for 5 days). The KOs spheroids have an increase of the area over time compared with the WT spheroids which have almost no alterations in their size. These results suggest that *LAMA2* deletion can influence the area of melanoma cell spheroids, and this influence is also pronounced over time.

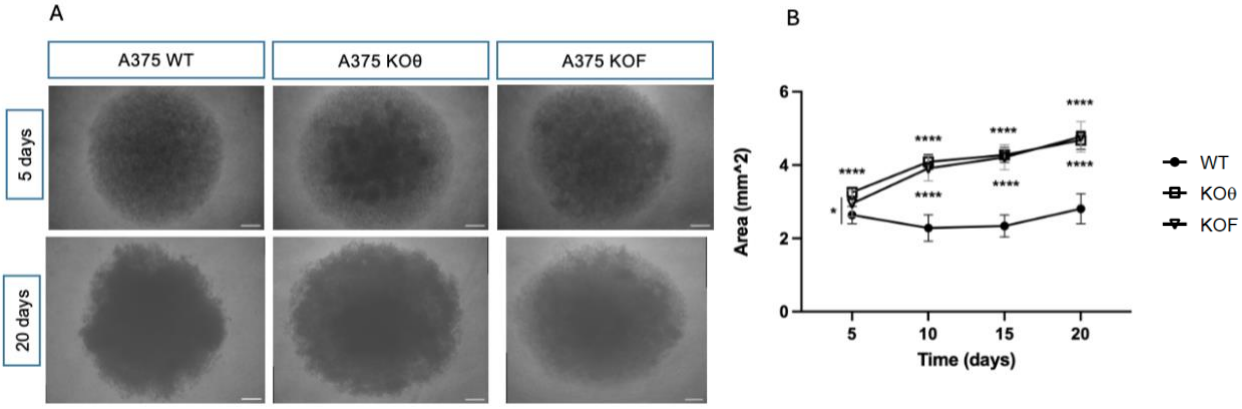

Figure 3.4: Absence of *LAMA2* increases melanoma spheroids area over time. A375 WT and KO cells were plated in a 96-well plate coated with 1% agarose in 1x PBS, at a concentration $5x10^5$ cells/mL. Two independent *LAMA2*-KO single clones were used KOθ and KOF. A drop of 20 µL were added to the well previously filled with 100 µL of DMEM. After, the plate was shacked in circular motion shaker to promote aggregation, during 10 minutes at 70 rpm. **(A)** Representative images of A375 WT and KO cells spheroids with 5 and 20 days. Amplification = 4x. Scale bar = 250 µm. **(B)** Measurement of spheroids area on days 5, 10, 15 and 20 post seeding for each cell line. ImageJ was used to measure spheroids area using brightfield images acquired on each timepoint. For each timepoint 4 spheroids were used to measure the area. N=3 independent experiments. Statistical analysis was performed by Two-way ANOVA with Dunnett's multiple comparisons test with *p-value < 0.05 and ****p-value < 0.0001.

In order to understand if the increase in spheroid size could be related to an increase in proliferation, Ki67 was analyzed in immunohistochemistry sections of WT and *LAMA2* KO spheroids. Although due to technical problems most of the samples were lost, except WT and KOθ spheroids with 10 days (**Figure 3.5**), a qualitative analysis of showed that Ki67 staining was mainly localized in cells at the

periphery of the spheroids, and pointed for a possible increase in the number of Ki67 positive cells in the WT spheroids.

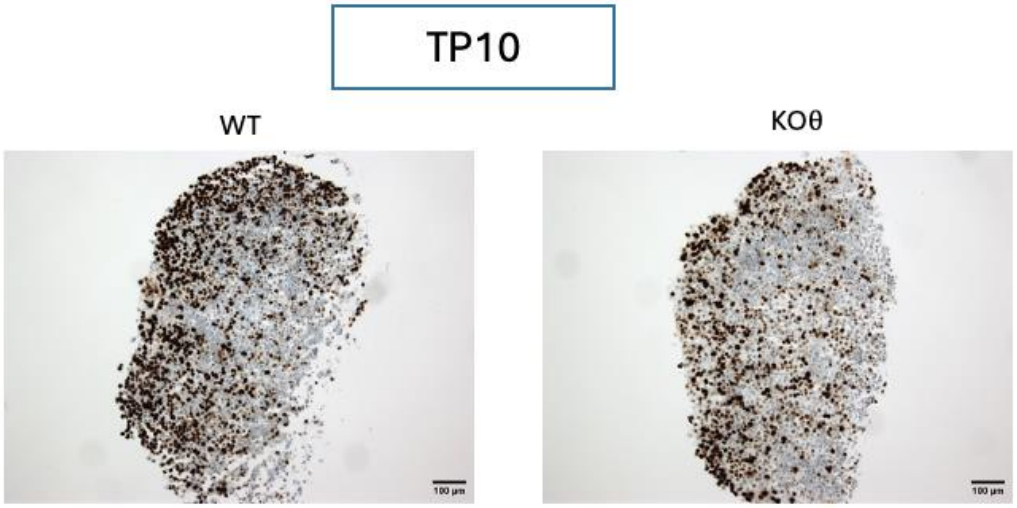

Figure 3.5: Ki67 staining in WT and KO spheroids with 10 days. A375 spheroids WT and KO cells were plated in a low attachment 96-well plates, filled with 100 µL of DMEM. Two independent *LAMA2*-KO single clones were used KOθ and KOF. A drop of 20 µL of a $5x10^5$ cells/mL concentration were added to the well. A375 WT and *LAMA2*-KO spheroids (with 5,10,15, and 20 days) were collected to HistoGel. After spheroids were fixed and embed in paraffin to performed slices of 4 µm. The slices were stained for Ki67. N=1 experiments. Amplification = 10x Scale bar: 100 µm.

Additionally, cleaved caspase-3 immunostaining was performed to detect apoptotic cells (**Figure 3.6**). Only spheroids from WT and KOθ cultured for 5, 10, and 20 days were analyzed, considering that other spheroids were lost due technical problems. Preliminary analysis suggests that WT and KOθ spheroids may have more signal for cleaved caspase-3 in spheroids cultured for 20 days than spheroids cultured for 5 or 10 days (**Figure 3.6**), in the images acquired in inner part of the spheroid. Nevertheless, no conclusion can be drawn from this staining.

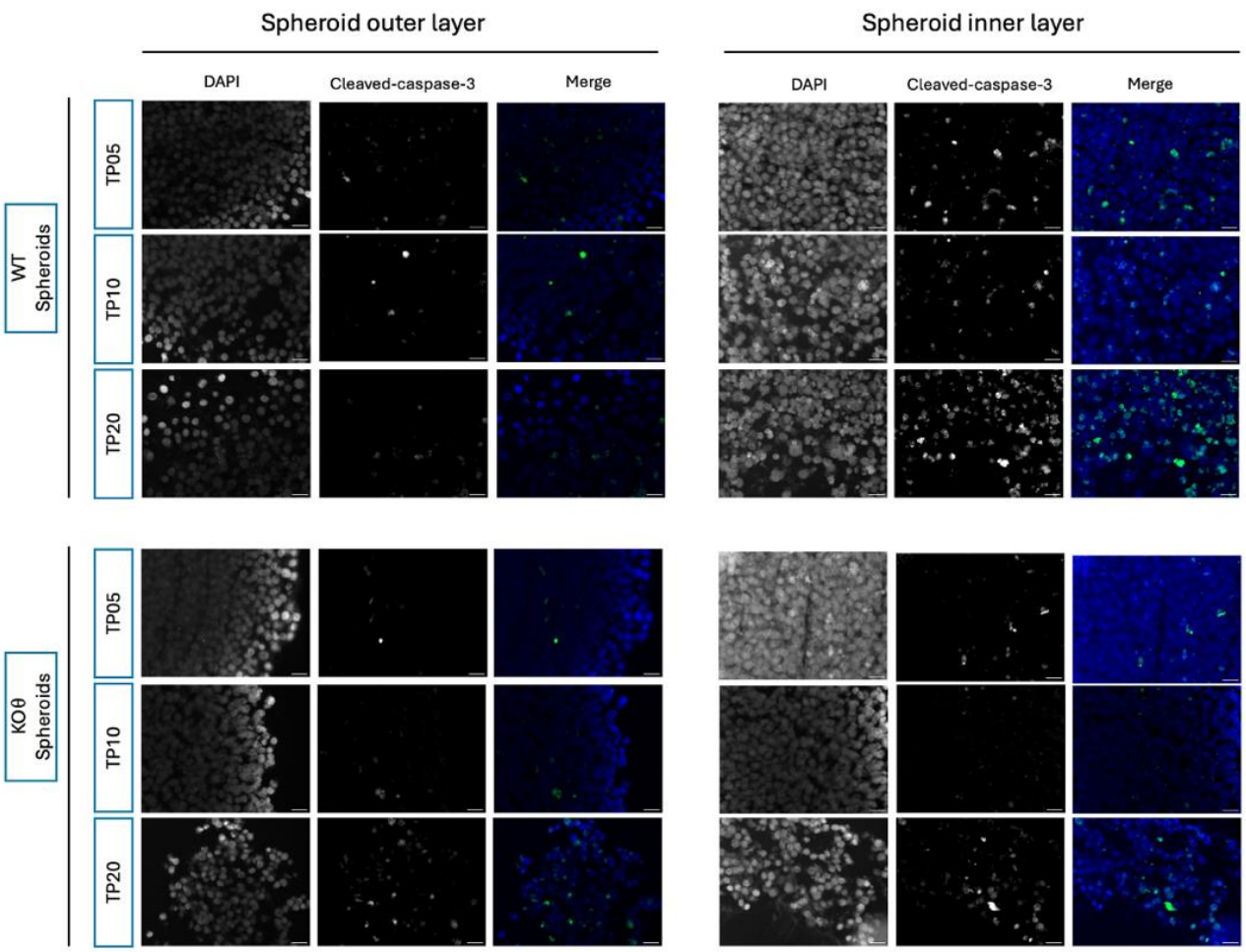

Figure 3.6: Cleaved caspase-3 signal in WT and KO θ spheroids sliced. A375 spheroids WT and KO cells were plated in a low attachment 96-well plates, filled with 100 µL of DMEM. Two independent LAMA2-KO single clones were used KOθ and KOF. A drop of 20 µL of a $5x10^5$ cells/mL concentration were added to the well. A375 WT and LAMA2-KO spheroids (with 5, 10, 15, and 20 days) were collected to HistoGel. After, spheroids were fixed and embed in paraffin to performed slices of 4 µm. The slices were stained for cleaved caspase-3. N=1 experiments. Amplification= 40x Scale bar: 20 µm.

3.3. *LAMA2*-deficiency affects *RAC1* gene expression in 2D melanoma cells

Given the importance of ECM on cell migration, the effects of *LAMA2* mutations on migratory capacity of melanoma were also analyzed. Previous results from the host laboratory showed a decrease in the migratory capacity of KO cells in comparison to WT cells, using 2D models[78]. To complement these results, the mRNA expression of two genes related with migration (*RAC1* and *TIMP1*) was analyzed. The results showed a downregulation of the expression of *RAC1* in KO cell lines, with a significant difference between WT and KOF (**Figure 3.7**). Regarding *TIMP1* there was also a tendency for a downregulation in KO cells, however the WT shows a high variation. These results suggest that absence of *LAMA2* alters the expression of *RAC1* and *TIMP1* in A375 melanoma cell line.

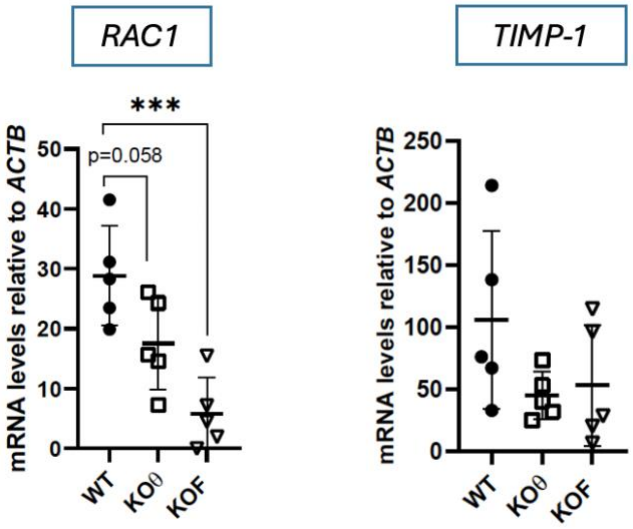

Figure 3.7: The absence of *LAMA2* impacts the expression of genes linked to migration in melanoma 2D cells. A375 cells WT and KO, two different single clones, were collected after performed scratch assay during 72h. The expression of genes related with migration were analyzed by qRT-PCR (*RAC1* and *TIMP1*). *ACTB*, encoding β-actin, was used as housekeeping gene. N=5 independent experiments. Statistical analysis was performed using One-way ANOVA with Dunnett´s multiple comparisons test ***$p < 0.001$.

3.4. Effects of *LAMA2* deletion on the migration of melanoma spheroids

To understand if *LAMA2* expression would also impact the migration of spheroids, WT and KO spheroids were transferred (at 5, 10, 15, and 20 days post seeding) to plates coated with gelatin to allow cells to migrate out from the spheroid. Then, migration was analyzed until 72 hours post-plating (**Figure 3.8A**). Images were acquired and analyzed using ImageJ, by drawing a line delimitating the core area (cells that do not migrate) and the total area (including cells that were migrating) (**Supplementary Figure 2**). The results (**Figure 3.8B**) showed that KOs spheroids have a tendency for a decreased migration capacity comparing with WT spheroids, that have a higher percentage of migration area during the 72h. This tendency can be observed in all the timepoints, except for spheroids cultured for 20 days (TP20), where the WT migration results was similar to the KOs spheroids.

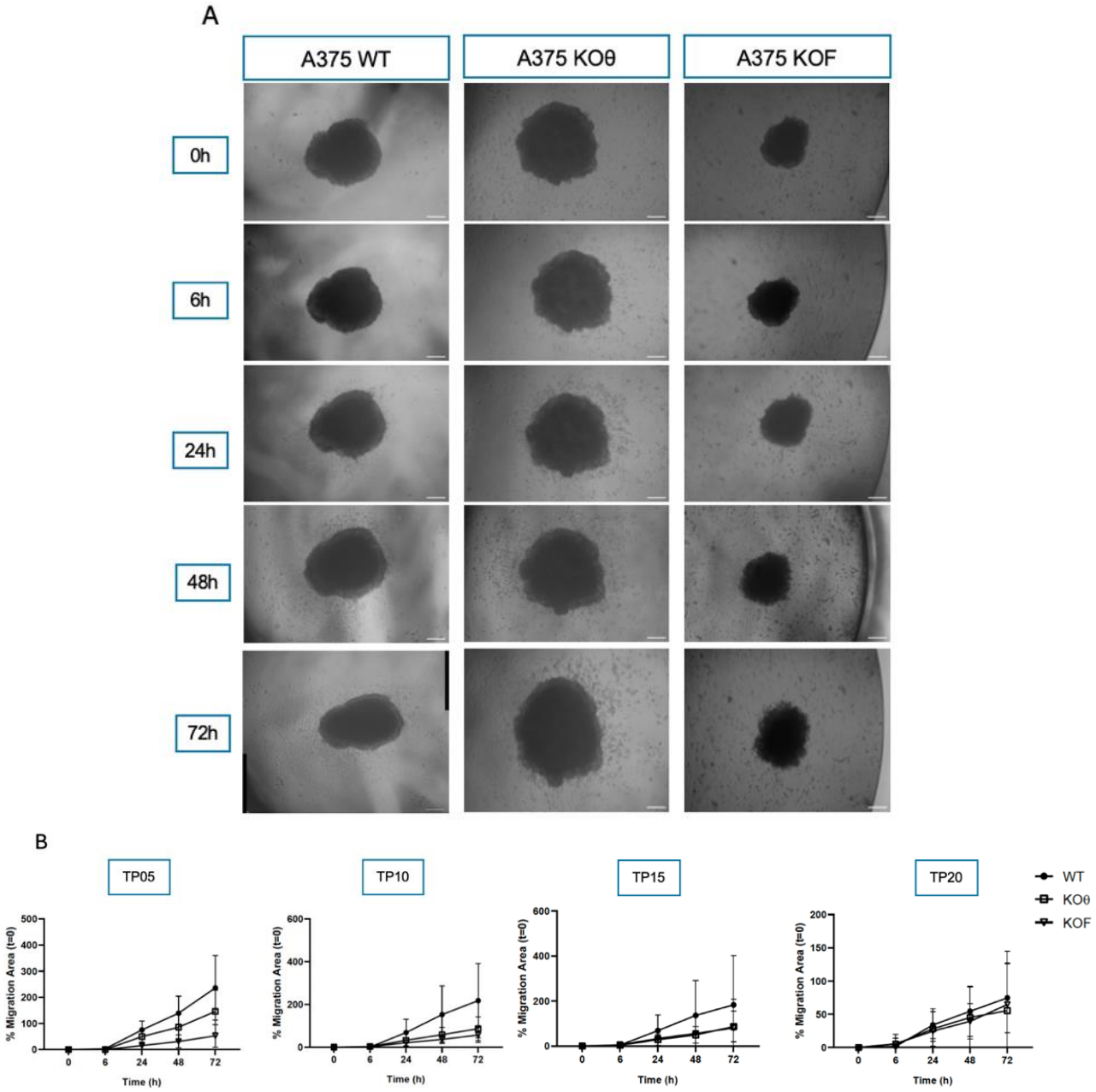

Figure 3.8: *LAMA2*-deficiency may decrease cell migration in melanoma spheroids. A375 WT and *LAMA2*-KO spheroids were plated and after 5, 10, 15, and 20 days post seeding (correspondent to TP05, TP10, TP15 and TP20, respectively), they were transferred into a 96- well plate previously coated with 0.1% gelatin and blocked with 1% BSA in 1x PBS. **(A)** Representative images of A375 WT and KO cells spheroids with 10 days during migration assay at 0, 6, 24, 48 and 72h after transferred to the migration plate. Amplification = 4x. Scale bar = 250 µm. **(B)** Quantification of the percentage of migration area during 72h from image as in A). The migration area was determined by the difference between the total area and the area of the core and then normalized to 0h timepoint. ImageJ was used to measure migration area using brightfield images acquire on each timepoint. Six spheroids were analyzed per cell line. N=3 independent experiments.

To analyze the migration results more easily and facilitate comparison between WT and KO, the area under the curve (AUC) was calculated and the results were plotted in next graph (**Figure 3.9**).

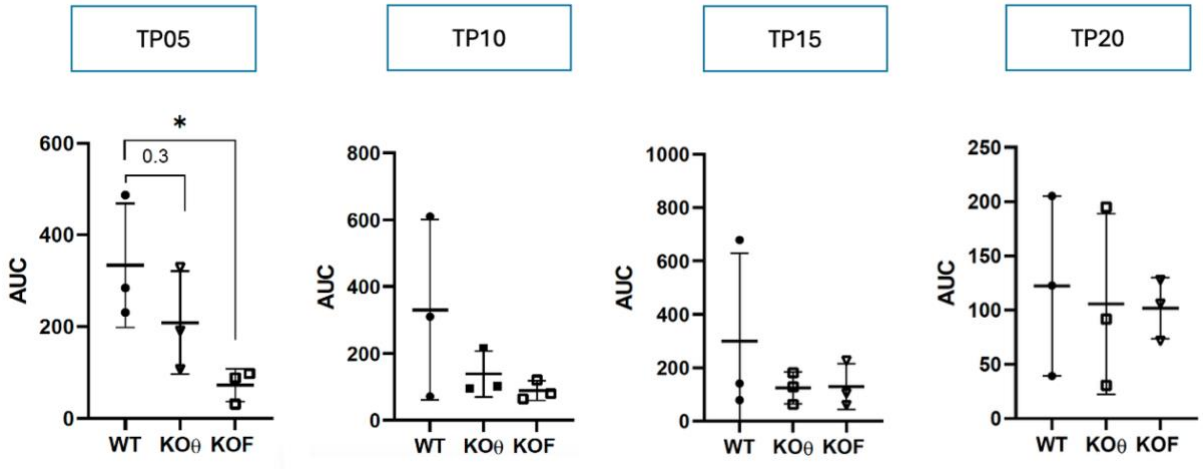

Figure 3.9: *LAMA2*-deficiency decrease cell migration in 5-days melanoma spheroids. From previous results (Figure 3.6) the area under the curve was analyzed and the results were plotted to summarize the overall migration behavior, since each point reflects the entire curve. N=3 independent experiments. Statistical analysis was performed using a One-way ANOVA with Dunnett's multiple comparisons test *p < 0.05.

In this analysis, each point reflects the entire curve, providing a summary of the migration behavior, allowing a straightforward comparison. In melanoma spheroids cultured for 5 days (TP05) there is a decrease of migration area in KO spheroids, with a significant difference between WT and KOF. For spheroids cultured for 10 days (TP10) there is also a tendency to a decreased of the migration on KO compared to WT. The KOθ and KOF spheroids seem to have similar results between biological replicates, however WT spheroids showed some variation between replicates. For TP15, that correspond to spheroids cultured for 15 days, the KO spheroids are again similar to each other, with low variation between replicates, but the WT spheroids seem to decrease the migration area, present also variation between replicates, and is not observed the same tendency that was in the TP05 and TP10. To finish, in spheroids with 20 days (TP20), there is an evident reduction of the AUC values for WT spheroids, and there are no differences between WT and KO spheroids.

To complement this analysis of the migration area and given that in 2D melanoma the analysis for *RAC1* and *TIMP-1* expression showed a tendency to be decreased in KO cells lines, these genes were also analyzed in spheroids. After the migration assay, WT and KO spheroids were collected and *RAC1* and *TIMP-1* gene expression were analyzed for each timepoint (5, 10, 15, and 20 days). Regarding *RAC1* gene expression, the results showed a significant difference in spheroids cultured for 10 days (TP10) with a downregulation of the *RAC1* gene in KO spheroids (**Figure 3.10A**). The WT spheroids cultured for 5 days (TP05) present variation between replicates. However, the KO spheroids present similar trends. For spheroids cultured for 15 and 20 days (TP15 and TP20) the replicates presented a variation and there were no differences between WT and KO spheroids.

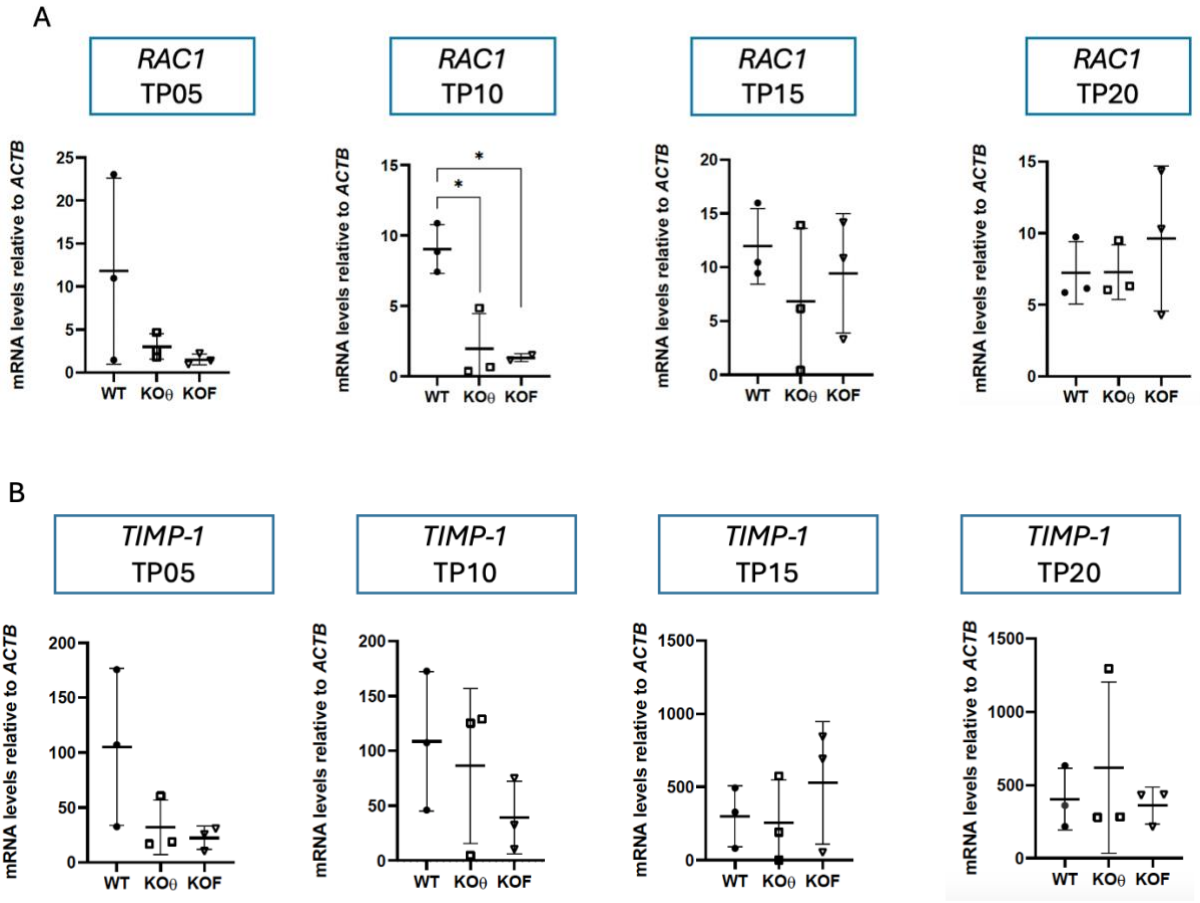

Figure 3.10: The absence of *LAMA2* may impact the expression of genes linked to migration in 10 days melanoma spheroids. A375 spheroids were collected after migrating during 72h, at each timepoint (TP5, TP10, TP15, TP20). The expression of genes related with migration process were analyzed by qRT-PCR (*RAC1* and *TIMP-1*). *ACTB*, encoding β-actin, was used as housekeeping gene. N=3, except for TP10 *RAC1* for KOF n=2, independent experiments. Statistical analysis was performed using a One-way ANOVA with Dunnett's multiple comparisons.

For *TIMP-1* gene expression analysis (**Figure 3.10B**) there were also no differences between WT and KO spheroids. However, it is possible to observe a tendency for a downregulation in spheroids cultured for 5 days (TP05), with WT spheroids showing variation in the results. For the other timepoints (10, 15, and 20 days) the results of WT and KO spheroids showed variation between replicates, but no tendency or differences were found. Overall, more samples should be added to these results to have a more robust analysis.

3.5. *LAMA2* deletion did not affect co-culture spheroids migration

In the context of the organism, cancer cells, such as melanoma cells, are surrounded by other types of cells. This surrounding environment, also called TME, interacts with cancer cells, and vice-versa. As already mentioned, these interactions can affect the tumor developments and progression[23]. One type of cells that is a component of the TME and has an important role, by remodeling the TME and communicate with cancer cells, are the fibroblasts. These cells can change their behavior promoting tumor progression. They can secrete growth factors that activate MAPK and AKT signaling pathways,

increasing migration[23] and they also may secrete MMPs that facilitate the migration of melanoma cells[79]. As shown before with monoculture migration assay, the KOs melanoma spheroids, cultured for 5 and 10 days, showed a tendency to have the lowest migration capacity, comparing with WT spheroids. The goal here was to understand if by doing a co-culture this migratory phenotype could be different. A co-culture of melanoma cells (WT and KOs) with Human Fetal Foreskin Fibroblast 2 (HFFF2) prepared and cultured for 5, 10, 15, and 20 days (same timepoints as in the monoculture). However, due to some technical problems, the co-cultured spheroids cultured for 15 and 20 days were lost, so it was only possible to analyze spheroids cultured for 5 and 10 days (TP05 and TP10, respectively).

When spheroids reached the timepoint of interest, they were transferred into a plate coated with gelatin to analyze migration, during 72h (**Figure 3.11A-C**), similar to what was done with the monoculture spheroids. To distinguish between the melanoma and fibroblast cells, the fibroblasts used in this experiment expressed GFP (GFP+ fibroblasts were produced by Vanessa Ribeiro). Observing the images is possible to see fibroblasts (green cells) **(Figure 3.11A-C**). Migration was analyzed by delimitating the core area (cells that do not migrate) and the total area (including cells that were migrating) (**Supplementary Figure 2).** The results did not show differences between WT and KO co-culture spheroids cultured for 5 or 10 days, as they seemed to have a similar migration profile during the time analyzed (**Figure 3.11D**).

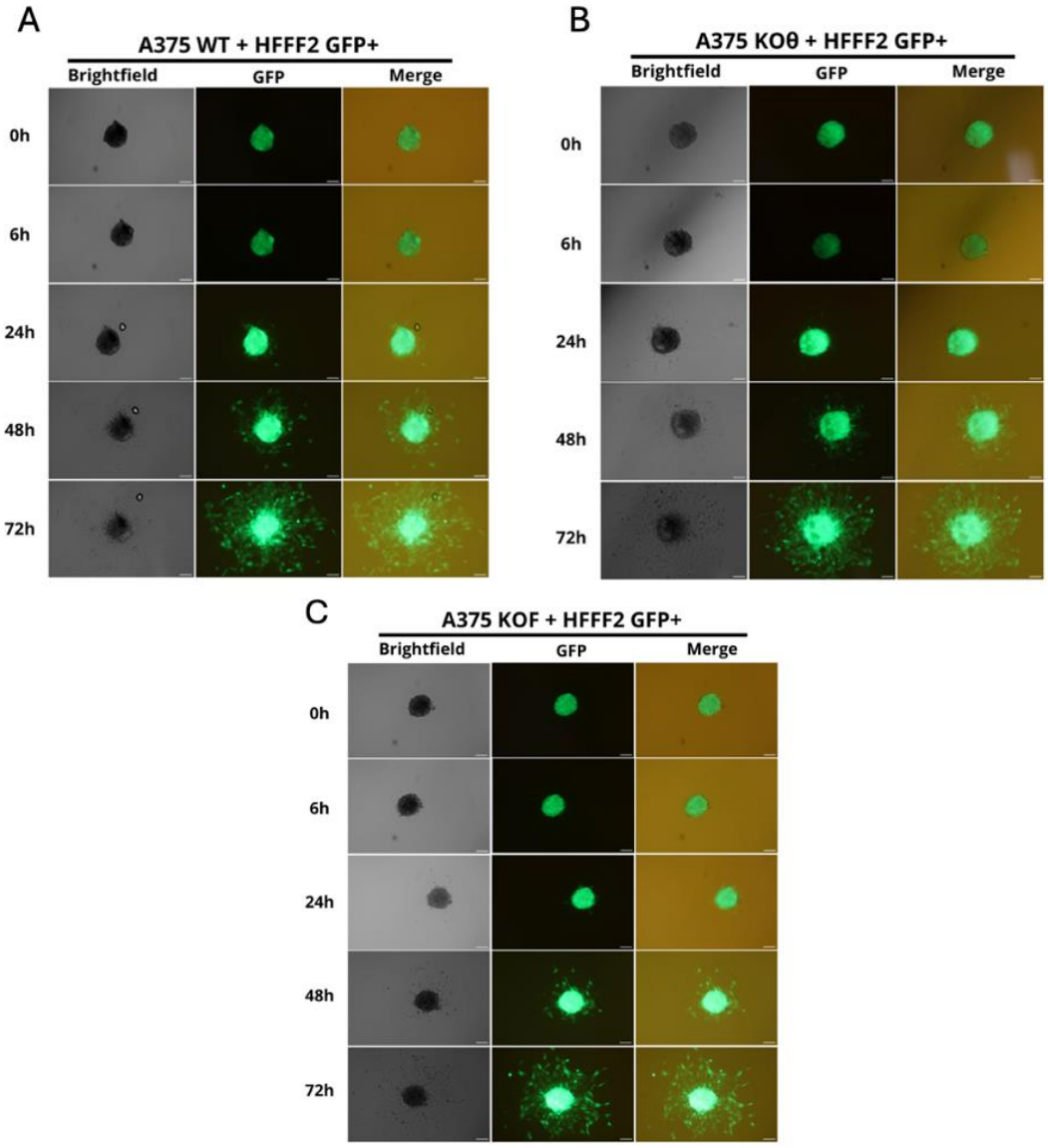

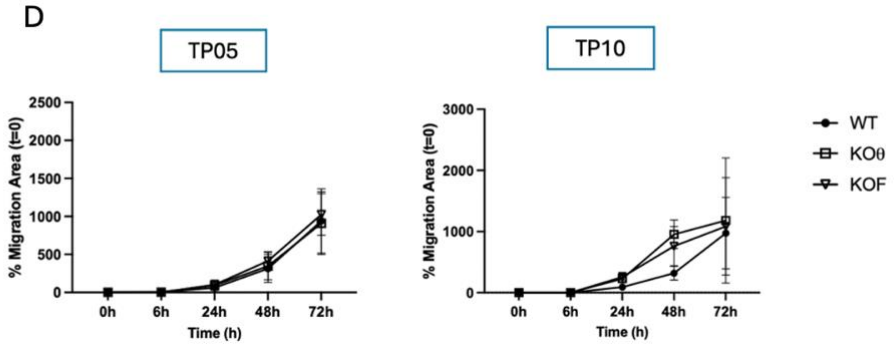

Figure 3.11: *LAMA2* deletion did not affect co-culture spheroids migration. WT HFFF2 fibroblasts were plated in 96-well plates previously coated with agarose 1% in 1x PBS, at a concentration $1x10^5$ cells/mL. A drop of 20 µL was added to the well previously filled with 100 µL of DMEM. The plate was set to shake in a circular motion shaker to promote aggregation, during 10 minutes at 70 rpm. After three days A375 WT and KO melanoma cells were added at a concentration of $2,5\ x10^3$ cells/mL, and the plate was once again put into motion. Spheroids grew for additional 5 days and then were transferred into a plate coated with 0.1% gelatin to evaluate migration at 0, 6, 24, 48 and 72 hours. **(A)** Representative images of co-cultured spheroids with melanoma WT cells and fibroblast **(B)** Representative images of co-cultured spheroids with melanoma *LAMA2*-KOθ cells and fibroblast **(C)** Representative images of co-cultured spheroids with melanoma *LAMA2*-KOF cells and fibroblast, with 5 days during migration assay at 0, 6, 24, 48 and 72h after transfer to the migration plate. Amplification = 10x. Scale bar = 100 µm. **(D)** Quantification of the percentage of migration area in co-culture spheroids with 5 and 10 days during 72h from image as represented in A), determined by the difference between the total area and the area of the core and then normalized to 0h timepoint. ImageJ was used to measure migration areas using brightfield images acquire on each timepoint. For migration analysis six spheroids were analyzed per cell line. N=1 experiments.

For this migration analysis the area under the curve (AUC) was calculated and the results were plot (**Figure 3.12**).

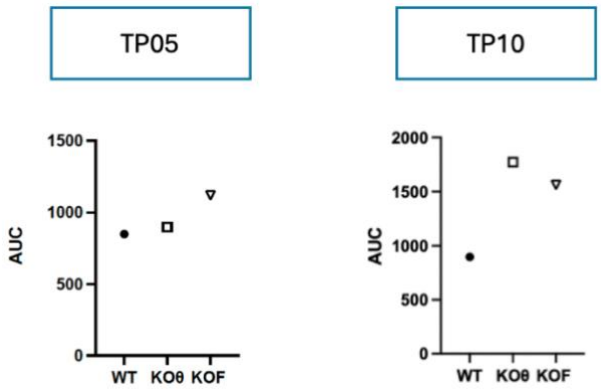

Figure 3.12: Co-culture of WT fibroblasts with *LAMA2*-deficient melanoma may contribute to an increase of migration in melanoma spheroids. From previous results (Figure 3.9) the area under the curve was analysis to summarize the overall migration behavior, and the results were plotted in this graphics, and each point reflects the entire curve. Results for timepoint day 5 (TP05) and day 10 (TP10) are shown. N=1 experiment.

From the AUC results, it seems that co-culture KO spheroids tend to migrate more than the WT co-culture spheroids, with a more pronounced tendency in spheroids cultured for 10 days (TP10) (which is contrary to what was seen in the monoculture). However, is important to consider that this analysis just has N=1 experiments, being necessary in the future to include more sets of samples to have more robust results and accurate conclusions.

4. Discussion

The TME has been recognized to play an integral role in tumorigenesis and malignant progression, contributing to several hallmarks of cancer[14,22]. The ECM, a key component of the TME, is present in all tissues and organs throughout the body[22], providing structural support and regulating essential cellular functions[31]. Cancer ECM differs from the ECM found in normal tissue in terms of composition, organization and physical and biochemical properties[22], which in the case of tumors are tailored to support cancer progression and metastasis[39]. In this project the aim was to understand how changes in the *LAMA2* gene, which encodes for the α2 chain of laminins, can affect melanoma progression. Previous unpublished results from the host laboratory suggested that the absence of *LAMA2* in a 2D model affects melanoma cells, reducing proliferation and migration, and increasing cell death and DNA damage[76,78]. Moreover, decreased proliferation and increased DNA damage was also found in C2C12 myoblasts (precursors of muscle fibers) lacking *Lama2*[48]. Together this suggests that the absence of laminin-α2 chain compromises different cellular processes, independently of the cell type.

Cancer cells, including melanoma cells, have a different behavior when cultured in 2D or 3D models[30]. This is probably due the fact that in 2D models, cells do not experience the same cell-cell and cell-ECM interactions, as well as the gradient of nutrients and oxygen, that occurs in 3D systems[30]. Since 3D culture systems have been shown to better stimulate the TME, and this project focuses on the consequences of the lack of an ECM component, it was important to use a model that facilitated cell-ECM interactions[73]. In this project, spheroids were produced using A375 WT and *LAMA2*-KO melanoma cell lines and different characteristics were analyzed at four different timepoints, 5, 10, 15, and 20 days post-seeding. Spheroids typically form three layers over time, a superficial layer, mainly containing cells in proliferation, an intermediate layer with cells in senescence/quiescent phase, and the core, the inner layer that predominantly contains cells in necrosis, but cells in apoptosis can also be found[75] (**Figure 1.3**). Previous studies analyzed A375 melanoma spheroids mainly between days 7 to 15, showing viability throughout this period[11,80,81]. To evaluate the impact of *LAMA2*-deficiency in the viability of spheroids, their area was measured. *LAMA2*-KO spheroids showed a significant increase in the area over time comparing with the WT spheroids (**Figure 3.4**). The WT spheroids did not show a big fluctuation in terms of area over time. These results may suggest that the absence of *LAMA2* seems to lead to an increase in the area of spheroids. One of the reasons that may explain the bigger area in KOs spheroids could be an increase in proliferation rate in *LAMA2*-KO spheroids, leading to a larger outer proliferative layer. This would contradict what was previously reported in a 2D A375 model, where *LAMA2*-deficiency correlated with a decrease in proliferation[78]. To test this hypothesis slices of spheroids were analyzed by immunohistochemistry using Ki67 (marker for cells in proliferation) and cleaved caspase 3 (apoptosis marker). Due to technical constrains it was not possible to draw conclusions from these experiments. Nevertheless, location of higher levels of Ki67 in the periphery and increased cleaved caspase 3 signal in the inner layer is in accordance with previous reports in the literature[69,71,75]. From the images acquired, there were no striking differences between WT and *LAMA2*-KO spheroids, even though is possible that day 10 WT spheroids display a higher number of cells in proliferation (**Figure 3.5**). In parallel, the analysis of p53 phosphorylation in spheroids was also performed and did not show differences between WT and KOs spheroids over time (**Figure 3.2**). However, the analysis of each specific timepoint showed a decrease of the p-p53 levels in KOF comparing with WT spheroids cultured for 10 days (TP10) (**Figure 3.3**). This result is the opposite of what was obtained in 2D cells[78] (unpublished results), which showed an increase of the p-p53 levels in the KOs cells. This difference between cells in 2D and 3D could be due to the architecture of the model, since the cells are in other conformation and this could influence their response to the DNA damage and/or their cell survival mechanims[82,83]. Previous studies have reported this difference between 2D and 3D model regarding drug response, showing that in a 3D model there is a decrease in p53 levels[82,83]. In addition to the architectural

changes, the ECM composition differs between 2D and 3D models[84], which could also influence the results between 2D and 3D models. Cell survival depends on multiple factors, including signals from cell–cell interactions and interactions with the ECM[65]. When these signals are interrupted, or when stressful conditions such as DNA damage occur, normal cells may undergo apoptosis. The loss of *LAMA2,* contributes to the loss in ECM linkage and may consequently cause stress[54] to the cells, which could lead to an increase in apoptosis. Nevertheless, for the period under analysis this could not be observed in spheroids, even though results in 2D[76,78] (**Figure 3.1B**) and 3D (Vanessa Ribeiro, unpublished data) suggest the presence of higher levels of DNA damage and/or chromosomal aberrations. Is possible that in *LAMA2*-KO spheroids other proteins may compensate for the absence of the laminin-α2 chain, maintaining an adequate ECM structure and prevent apoptosis.

Since collectively the results did not indicate that absence of *LAMA2* could promote spheroid proliferation, and therefore this would not be the explanation for the increased area in *LAMA2*-KO spheroids. Another possibility that should be explored in the future is cell adhesion, which may differ between WT and *LAMA2* spheroids, as suggested by data on *LAMA2*-congenital muscular dystrophy[85].

In addition to alterations in proliferation, cell migration is yet another important process that might be compromised in the absence of *LAMA2*. The dynamic interaction between cells and the ECM is a key factor that drive cancer cells to migrate, contributing to tumor progression (migration processes generally coincide with the switch to malignant phase)[86,77]. The migration results of spheroids cultured for 5 days in culture showed a significant decrease of the percentage of migration in *LAMA2* KOF spheroids, and a tendency for *LAMA2* KOθ, when compared to the WT ones (**Figure 3.8**). In spheroids cultured for 10 days there was also a tendency for both KOθ and KOF to have a decrease in migration. These results are in accordance with 2D results, where the absence of *LAMA2* led to a decrease in the migration of melanoma cells[78]. In spheroids cultured for 15 and 20 days this tendency was lost, and there is no difference between WT and *LAMA2*-KO spheroids. Over time, there was a decrease in migration within the same cell line. For example, for WT spheroids, percentage of migration area is above 200% for day 5, while at day 20 the percentage of migration area drops below 100% (**Figure 3.8**). Previous studies have shown that time in culture could influence the capacity of cell migration[87], with data showing that migration increases with the age of the spheroids. Nevertheless, they did not used spheroids cultured for more than 11 days[87]. As suggested by the cleaved caspase-3 staining (**Figure 3.6**), spheroids cultured for 20 days may exhibit an increase in cell death, and this could explain the decreased in migration. In the future, it will be important to clarify this further with more detailed analysis of cell death in spheroids cultured for 5, 10, 15, and 20 days. Additionally, the results of spheroids cultured for 5 and 10 days could be explained by the important role that laminins play in cell migration[38], particularly *LAMA2* that contributes to stabilization of cell structure and mediate integrin signaling, which allows the activation of various cellular processes such as those promoting cell migration[42]. Moreover, laminin-211(LN211) contributes directly to cell migration through different mechanisms including: i) regulation of cellular pathways, including FAK regulation of cell adhesion dynamics and Rho GTPases activity[88,89]; ii) providing a gradient of LN211 (haptotactic effect) that serves as a directional cue for cell migration[90]. In cancer, migration can be activated by important pathways that are related to the cytoskeletal stabilization and mechanosensing[32], such as the activation of the Rho GTPase RAC1, which promotes cell migration, having an important role in lamellipodia formation[38]. Considering the defective migration of *LAMA2*-KO spheroids, it was hypothesized that *RAC1* expression could also be reduced. Indeed, the gene expression of *RAC1* was significantly downregulated in KOs spheroids cultured for 10 days (TP10), compared with WT spheroids (**Figure 3.10A**). The same tendency was observed for the 5 days timepoint, even though the difference was not significant. These results are in line with the hypothesis that *LAMA2*-defiency may affect migration and impact the expression of the *RAC1* gene. This was observed not only in spheroids but also in 2D, where analysis of *RAC1* expression in WT and KOs cell lines showed a downregulation of *RAC1* in KOs cell lines (with a significant downregulation in KOF)

(**Figure 3.7**). Additionally, wound healing assays previously performed by members of laboratory showed a significant decrease in migration capacity of the *LAMA2* KOs in comparison with WT cells[78]. The requirement of functional laminin for proper *RAC1* activation and migration has also been reported in other models, including a previous study in mouse embryonic stem cells (mESCs), showing that migration was stimulated by laminins through Rac1/cdc42/FAK pathways[91]. Also, another study using Schwann cells showed a decrease of *RAC1* and *cdc42* in the context of laminin deficiency[92], which was due to the role of laminins in coordinating the β1-integrin-RAC1 signaling pathway[92]. Additionally, some recent studies showed a relation between p53 and the motility of cancer cells by negatively modulating Rho GTPases, which regulate important cytoskeletal pathways vital for migration[93,94,95]. Rac, cdc42 and Rho are members of this family, responsible for actin dynamics and are integral to cytoskeletal changes. Regarding the *RAC1* gene, some studies report an inhibition by p53. A study in B- and T- lymphoma cells showed that *RAC1* activity was inversely regulated by p53[96], however the mechanisms are not clear[97,98]. These results seem to be in accordance with the results obtained for 2D, since the KO melanoma cells showed a tendency for a higher level of p53[78] and an inverse tendency for *RAC1* expression (**Figure 3.7**). However, in spheroids this pathway might not be activated in the same manner since at 10 days post seeding, *LAMA2*-KO spheroids present both a decrease in p-p53 phosphorylation (**Figure 3.3)** and in *RAC1* mRNA expression (**Figure 3.10A**). This highlights the differences between both models and the importance of developing models closer to the *in vivo* environment.

It has been described that cells have two different modes of invasion, namely proteolytic and non-proteolytic (amoeboid)[84]. Proteolytic invasion leads to structural remodeling of the ECM and degradation by proteases, such as MMPs. In non-proteolytic invasion, usually in softer matrixes, cells migrate by squeezing through the pores of the ECM without remodeling it and with a minimal proteolytic activity[99]. TIMP-1 is an inhibitor of MMP and therefore plays an important role in the regulation of cell migration[100]. The results obtained in the scope of this thesis showed that *TIMP-1* expression was not significantly different between WT and KO spheroids (**Figure 3.10B**). Since in these experiments melanoma cells migrated across a surface which did not require a degradation of a complex ECM, the proteolytic activity might be reduced, and therefore MMP synthesis and their inhibitors (such as *TIMP-1*) may not have been strongly induced. Nevertheless, future studies will be needed, such as the quantification of MMP expression, and the MMP/TIMP ratio in WT and *LAMA2*-KO spheroids. Additionally, it would be important to perform a 3D invasion assay to analyze if, under these conditions the absence of *LAMA2* can also affect the invasion of melanoma cells and alter protease-dependent invasion.

As mentioned before, the TME is composed of cell types other than cancer cells, which contribute to tumor progression. The TME of melanoma is formed not only by malignant cells but also complex interactions with non-cancerous cells such as fibroblasts, that participate in melanoma progression[30]. Fibroblasts are known to contribute to tumor progression providing signals that lead to the ECM remodeling and influence migration and invasion of melanoma cells[23]. In this project melanoma cell lines (WT and KOs) were cultured together with fibroblasts as part of co-culture spheroids. Since migration was the characteristic that led to clear differences between WT and *LAMA2* KO spheroids, migration was also analyzed to understand if, by co-culturing the cells, the migration would be altered. The migration of co-culture spheroids with fibroblasts and WT melanoma or fibroblasts and KO melanoma cells was analyzed, and the results showed that there are no significant differences in the percentage of migration area (**Figure 3.11D**). Analysis of the AUC revealed that KO co-culture spheroids have a tendency for an increased migration compared to WT co-culture spheroids (**Figure 3.12**), but it should be stressed that a reduced number of experiments were performed. To draw deeper conclusion about this in the future, it is necessary to increase the number of samples and it would be better to also fluorescently label also the melanoma cells, to better distinguish between melanoma cells

and fibroblasts and be able to assess if the KO cells are migrating more or less than the WT melanoma cells. Altogether, these results suggest that absence of the *LAMA2* gene can influence melanoma cells, in 2D and 3D *in vitro* models. The results showed a decrease in the migration capacity of the melanoma KO cell lines regardless of the model used. These results are in accordance with previous studies, which showed that, in bladder cancer cells, depletion of *LAMA2* inhibited migration and promoted apoptosis, contributing to a weakened invasiveness of the cells[50]. However, in breast cancer cells, the absence of *LAMA2* promotes invasiveness[50] and in PiNET the decrease of *LAMA2* leads to an increase of aggressiveness[42]. This could suggest that the role of *LAMA2* could be tumor-specific or even dependent on the stage of the tumor. In melanoma, the results suggest that the absence of *LAMA2* could lead to a decrease in cells aggressiveness. However more studies are needed to obtain more robust results.
Overall, this study investigated how the ECM component *LAMA2* affects melanoma progression, particularly in relation to cell migration and *RAC1* regulation, emphasizing the role of the ECM within the TME. By comparing 2D and 3D spheroid models, it highlights the relevance of using systems that are physiologically closer systems to the *in vivo* situation, to better capture cancer cell behavior and to explore ECM-related mechanisms that may contribute to melanoma development.

5. References

1. International Agency for Research on Cancer. Cancer Today: Melanoma of skin — Incidence (%) by world region (2022). World Health Organization; 2024 Feb. Available from:https://gco.iarc.fr/today/en/dataviz/pie?mode=population&cancers=16&group_populations=0

2. O'Neill CH, Scoggins CR. Melanoma. J Surg Oncol. 2019 Oct;120(5):873–81.

3. Schadendorf D, Van Akkooi ACJ, Berking C, Griewank KG, Gutzmer R, Hauschild A, et al. Melanoma. The Lancet. 2018 Sept;392(10151):971–84.

4. Bertolotto C. Melanoma: From Melanocyte to Genetic Alterations and Clinical Options. Scientifica. 2013 Nov;2013:1–22.

5. Uong A, Zon LI. Melanocytes in development and cancer. J Cell Physiol. 2010 Jan;222(1):38–41.

6. Shain AH, Bastian BC. From melanocytes to melanomas. Nat Rev Cancer. 2016 June;16(6):345–58.

7. Bento-Lopes L, Cabaço LC, Charneca J, Neto MV, Seabra MC, Barral DC. Melanin's Journey from Melanocytes to Keratinocytes: Uncovering the Molecular Mechanisms of Melanin Transfer and Processing. Int J Mol Sci. 2023 July 10;24(14):11289.

8. Brenner M, Hearing VJ. The Protective Role of Melanin Against UV Damage in Human Skin†. Photochem Photobiol. 2008 May;84(3):539–49.

9. Shreberk-Hassidim R, Ostrowski SM, Fisher DE. The Complex Interplay between Nevi and Melanoma: Risk Factors and Precursors. Int J Mol Sci. 2023 Feb 10;24(4):3541.

10. Davis EJ, Johnson DB, Sosman JA, Chandra S. Melanoma: What do all the mutations mean? Cancer. 2018 Sept;124(17):3490–9.

11. Fontana F, Sommariva M, Anselmi M, Bianchi F, Limonta P, Gagliano N. Differentiation States of Phenotypic Transition of Melanoma Cells Are Revealed by 3D Cell Cultures. Cells. 2024 Jan 17;13(2):181.

12. Hossain SM, Eccles MR. Phenotype Switching and the Melanoma Microenvironment; Impact on Immunotherapy and Drug Resistance. Int J Mol Sci. 2023 Jan 13;24(2):1601.

13. Nistico P, Bissell MJ, Radisky DC. Epithelial-Mesenchymal Transition: General Principles and Pathological Relevance with Special Emphasis on the Role of Matrix Metalloproteinases. Cold Spring Harb Perspect Biol. 2012 Feb 1;4(2):a011908–a011908.

14. Hanahan D. Hallmarks of Cancer: New Dimensions. Cancer Discov. 2022 Jan 1;12(1):31–46.

15. Tang Y, Durand S, Dalle S, Caramel J. EMT-Inducing Transcription Factors, Drivers of Melanoma Phenotype Switching, and Resistance to Treatment. 2020 Aug;12:2154.

16. Grzywa TM, Paskal W, Włodarski PK. Intratumor and Intertumor Heterogeneity in Melanoma. Transl Oncol. 2017 Dec;10(6):956–75.

17. Ramón Y Cajal S, Sesé M, Capdevila C, Aasen T, De Mattos-Arruda L, Diaz-Cano SJ, et al. Clinical implications of intratumor heterogeneity: challenges and opportunities. J Mol Med. 2020 Feb;98(2):161–77.

18. Wellbrock C, Rana S, Paterson H, Pickersgill H, Brummelkamp T, Marais R. Oncogenic BRAF Regulates Melanoma Proliferation through the Lineage Specific Factor MITF. Williams S, editor. PLoS ONE. 2008 July 16;3(7):e2734.

19. Ferguson J, Smith M, Zudaire I, Wellbrock C, Arozarena I. Glucose availability controls ATF4-mediated MITF suppression to drive melanoma cell growth. Oncotarget. 2017 May 16;8(20):32946–59.

20. Chang J, Campbell-Hanson KR, Vanneste M, Bartschat NI, Nagel R, Arnadottir AK, et al. Antagonistic roles for MITF and TFE3 in melanoma plasticity. Cell Rep. 2025 Apr;44(4):115474.

21. Popovic A, Tartare-Deckert S. Role of extracellular matrix architecture and signaling in melanoma therapeutic resistance. Front Oncol. 2022 Sept 2;12:924553.

22. Naser R, Fakhoury I, El-Fouani A, Abi-Habib R, El-Sibai M. Role of the tumor microenvironment in cancer hallmarks and targeted therapy (Review). Int J Oncol. 2022 Dec 27;62(2):23.

23. Romano V, Belviso I, Venuta A, Ruocco MR, Masone S, Aliotta F, et al. Influence of Tumor Microenvironment and Fibroblast Population Plasticity on Melanoma Growth, Therapy Resistance and Immunoescape. Int J Mol Sci. 2021 May 17;22(10):5283.

24. De Visser KE, Joyce JA. The evolving tumor microenvironment: From cancer initiation to metastatic outgrowth. Cancer Cell. 2023 Mar;41(3):374–403.

25. Javaid S, Zhang J, Anderssen E, Black JC, Wittner BS, Tajima K, et al. Dynamic Chromatin Modification Sustains Epithelial-Mesenchymal Transition following Inducible Expression of Snail-1. Cell Rep. 2013 Dec;5(6):1679–89.

26. Li G, Satyamoorthy K, Herlyn M. N-Cadherin-mediated Intercellular Interactions Promote Survival and Migration of Melanoma Cells. 2001 Feb;61:3819–25.

27. Busse A, Keilholz U. Role of TGF- β in Melanoma. Curr Pharm Biotechnol. 2011 Dec;12(12):2165–75.

28. Bellei B, Migliano E, Picardo M. A Framework of Major Tumor-Promoting Signal Transduction Pathways Implicated in Melanoma-Fibroblast Dialogue. Cancers. 2020 Nov 17;12(11):3400.

29. Legrand M, Mousson A, Carl P, Rossé L, Justiniano H, Gies JP, et al. Protein dynamics at invadopodia control invasion–migration transitions in melanoma cells. Cell Death Dis. 2023 Mar 11;14(3):190.

30. Maria Hölken J, Elisabeth Teusch N. Recent developments of 3D models of the tumor microenvironment for cutaneous melanoma: Bridging the gap between the bench and the bedside? J Transl Sci. 2021;7(1).

31. Karamanos NK, Theocharis AD, Piperigkou Z, Manou D, Passi A, Skandalis SS, et al. A guide to the composition and functions of the extracellular matrix. FEBS J. 2021 Dec;288(24):6850–912.

32. Winkler J, Abisoye-Ogunniyan A, Metcalf KJ, Werb Z. Concepts of extracellular matrix remodelling in tumour progression and metastasis. Nat Commun. 2020 Oct 9;11(1):5120.

33. Chang J, Chaudhuri O. Beyond proteases: Basement membrane mechanics and cancer invasion. J Cell Biol. 2019 Aug 5;218(8):2456–69.

34. Mayasin YP, Osinnikova MN, Kharisova CB, Kitaeva KV, Filin IY, Gorodilova AV, et al. Extracellular Matrix as a Target in Melanoma Therapy: From Hypothesis to Clinical Trials. Cells. 2024 Nov 19;13(22):1917.

35. Nonnast E, Mira E, Mañes S. Biomechanical properties of laminins and their impact on cancer progression. Biochim Biophys Acta BBA - Rev Cancer. 2024 Nov;1879(6):189181.

36. McCarthy JB, Furcht LT. Laminin and fibronectin promote the haptotactic migration of B16 mouse melanoma cells in vitro. J Cell Biol. 1984 Apr 1;98(4):1474–80.

37. Chang J, Chaudhuri O. Beyond proteases: Basement membrane mechanics and cancer invasion. J Cell Biol. 2019 Aug 5;218(8):2456–69.

38. Nonnast E, Mira E, Mañes S. Biomechanical properties of laminins and their impact on cancer progression. Biochim Biophys Acta BBA - Rev Cancer. 2024 Nov;1879(6):189181.

39. Prakash J, Shaked Y. The Interplay between Extracellular Matrix Remodeling and Cancer Therapeutics. Cancer Discov. 2024 Aug 2;14(8):1375–88.

40. Aumailley M. Laminins and interaction partners in the architecture of the basement membrane at the dermal-epidermal junction. Exp Dermatol. 2021 Jan;30(1):17–24.

41. Napolitano F, Fabozzi M, Montuori N. Non-Integrin Laminin Receptors: Shedding New Light and Clarity on Their Involvement in Human Diseases. Int J Mol Sci. 2025 Apr 10;26(8):3546.

42. Hu J, Li S. The Role of Lama2 in Cancer: Current Perspectives. 2022 Nov;10(4):85–8.

43. Oikawa Y, Hansson J, Sasaki T, Rousselle P, Domogatskaya A, Rodin S, et al. Melanoma cells produce multiple laminin isoforms and strongly migrate on α5 laminin(s) via several integrin receptors. Exp Cell Res. 2011 May;317(8):1119–33.

44. Akhavan A, Griffith OL, Soroceanu L, Leonoudakis D, Luciani-Torres MG, Daemen A, et al. Loss of Cell-Surface Laminin Anchoring Promotes Tumor Growth and Is Associated with Poor Clinical Outcomes. Cancer Res. 2012 May 15;72(10):2578–88.

45. Liang J, Oyang L, Rao S, Han Y, Luo X, Yi P, et al. Rac1, A Potential Target for Tumor Therapy. Front Oncol. 2021 May 17;11.

46. Colón-Bolea P, García-Gómez R, Casar B. RAC1 Activation as a Potential Therapeutic Option in Metastatic Cutaneous Melanoma. Biomolecules. 2021 Oct 20;11(11):1554.

47. Yurchenco PD, McKee KK, Reinhard JR, Rüegg MA. Laminin-deficient muscular dystrophy: Molecular pathogenesis and structural repair strategies. Matrix Biol. 2018 Oct;71–72:174–87.

48. Martins SG, Ribeiro V, Melo C, Paulino-Cavaco C, Antonini D, Naidu SD, et al. Deregulation of multiple mechanisms shapes the onset of *LAMA2* -congenital muscular dystrophy. Developmental Biology; 2024.

49. Nguyen Q, Lim KRQ, Yokota T. Current understanding and treatment of cardiac and skeletal muscle pathology in laminin-α2 chain-deficient congenital muscular dystrophy. Appl Clin Genet. 2019 July;Volume 12:113–30.

50. Jin Y, Huang S, Wang Z. Identify and validate RUNX2 and LAMA2 as novel prognostic signatures and correlate with immune infiltrates in bladder cancer. Front Oncol. 2023 July 13;13:1191398.

51. Patton BL, Wang B, Tarumi YS, Seburn KL, Burgess RW. A single point mutation in the LN domain of LAMA2 causes muscular dystrophy and peripheral amyelination. J Cell Sci. 2008 May 15;121(10):1593–604.

52. De Bernabé DBV, Inamori K ichiro, Yoshida-Moriguchi T, Weydert CJ, Harper HA, Willer T, et al. Loss of α-Dystroglycan Laminin Binding in Epithelium-derived Cancers Is Caused by Silencing of LARGE. J Biol Chem. 2009 Apr;284(17):11279–84.

53. Oikawa Y, Hansson J, Sasaki T, Rousselle P, Domogatskaya A, Rodin S, et al. Melanoma cells produce multiple laminin isoforms and strongly migrate on α5 laminin(s) via several integrin receptors. Exp Cell Res. 2011 May;317(8):1119–33.

54. Martins SG, Zilhão R, Thorsteinsdóttir S, Carlos AR. Linking Oxidative Stress and DNA Damage to Changes in the Expression of Extracellular Matrix Components. Front Genet. 2021 July 29;12:673002.

55. Gawlik KI, Körner Z, Oliveira BM, Durbeej M. Early skeletal muscle pathology and disease progress in the dy3K/dy3K mouse model of congenital muscular dystrophy with laminin α2 chain-deficiency. Sci Rep. 2019 Oct 4;9(1):14324.

56. M. Harandi V, Moreira Soares Oliveira B, Allamand V, Friberg A, Fontes-Oliveira CC, Durbeej M. Antioxidants Reduce Muscular Dystrophy in the dy2J/dy2J Mouse Model of Laminin α2 Chain-Deficient Muscular Dystrophy. Antioxidants. 2020 Mar 18;9(3):244.

57. Tiwari V, Wilson DM. DNA Damage and Associated DNA Repair Defects in Disease and Premature Aging. Am J Hum Genet. 2019 Aug;105(2):237–57.

58. Corti A, Duarte TL, Giommarelli C, De Tata V, Paolicchi A, Jones GDD, et al. Membrane gamma-glutamyl transferase activity promotes iron-dependent oxidative DNA damage in melanoma cells. Mutat Res Mol Mech Mutagen. 2009 Oct;669(1–2):112–21.

59. Vlašić I, Horvat A, Tadijan A, Slade N. p53 Family in Resistance to Targeted Therapy of Melanoma. Int J Mol Sci. 2022 Dec 21;24(1):65.

60. Williams AB, Schumacher B. p53 in the DNA-Damage-Repair Process. Cold Spring Harb Perspect Med. 2016 May;6(5):a026070.

61. Box NF, Vukmer TO, Terzian T. Targeting p53 in melanoma. Pigment Cell Melanoma Res. 2014 Jan;27(1):8–10.

62. Lu M, Miller P, Lu X. Restoring the tumour suppressive function of p53 as a parallel strategy in melanoma therapy. FEBS Lett. 2014 Aug 19;588(16):2616–21.

63. Deng M, Lin J, Nowsheen S, Liu T, Zhao Y, Villalta PW, et al. Extracellular matrix stiffness determines DNA repair efficiency and cellular sensitivity to genotoxic agents. Sci Adv. 2020 Sept 11;6(37):eabb2630.

64. Li LN, Wang DR, Sato M, Kojima N, Imai K, Higashi N, et al. Extracellular matrix-regulated p53 expression and nuclear localization in cultured Detroit 562 cells derived from pharyngeal carcinoma. Arch Histol Cytol. 2003;66(5):419–28.

65. Ilić D, Almeida EAC, Schlaepfer DD, Dazin P, Aizawa S, Damsky CH. Extracellular Matrix Survival Signals Transduced by Focal Adhesion Kinase Suppress p53-mediated Apoptosis. J Cell Biol. 1998 Oct 19;143(2):547–60.

66. Muller PAJ, Vousden KH, Norman JC. p53 and its mutants in tumor cell migration and invasion. J Cell Biol. 2011 Jan 24;192(2):209–18.

67. Ferreira D, Adega F, Chaves R. The Importance of Cancer Cell Lines as in vitro Models in Cancer Methylome Analysis and Anticancer Drugs Testing. In: Lopez-Camarillo C, editor. Oncogenomics and Cancer Proteomics - Novel Approaches in Biomarkers Discovery and Therapeutic Targets in Cancer. InTech; 2013.

68. Jensen C, Teng Y. Is It Time to Start Transitioning From 2D to 3D Cell Culture? Front Mol Biosci. 2020 Mar 6;7:33.

69. Nascentes Melo LM, Kumar S, Riess V, Szylo KJ, Eisenburger R, Schadendorf D, et al. Advancements in melanoma cancer metastasis models. Pigment Cell Melanoma Res. 2023 Mar;36(2):206–23.

70. Fontoura JC, Viezzer C, Dos Santos FG, Ligabue RA, Weinlich R, Puga RD, et al. Comparison of 2D and 3D cell culture models for cell growth, gene expression and drug resistance. Mater Sci Eng C. 2020 Feb;107:110264.

71. Boussommier-Calleja A. In vitro models of cancer. In: Bioengineering Innovative Solutions for Cancer. Elsevier; 2020. p. 273–325.

72. Imamura Y, Mukohara T, Shimono Y, Funakoshi Y, Chayahara N, Toyoda M, et al. Comparison of 2D- and 3D-culture models as drug-testing platforms in breast cancer. Oncol Rep. 2015 Apr;33(4):1837–43.

73. Nayak P, Bentivoglio V, Varani M, Signore A. Three-Dimensional In Vitro Tumor Spheroid Models for Evaluation of Anticancer Therapy: Recent Updates. Cancers. 2023 Oct 4;15(19):4846.

74. Zhu Y, Kang E, Wilson M, Basso T, Chen E, Yu Y, et al. 3D Tumor Spheroid and Organoid to Model Tumor Microenvironment for Cancer Immunotherapy. Organoids. 2022 Dec 5;1(2):149–67.

75. Garnique ADMB, Parducci NS, De Miranda LBL, De Almeida BO, Sanches L, Machado-Neto JA. Two-Dimensional and Spheroid-Based Three-Dimensional Cell Culture

Systems: Implications for Drug Discovery in Cancer. Drugs Drug Candidates. 2024 June 13;3(2):391–409.

76. Fonseca I. Characterizing the impact of LAMA2-deficiency in cancer cell lines [Master thesis]. Faculty od Sciences of University of Lisbon; 2023.

77. Vinci M, Box C, Zimmermann M, Eccles SA. Tumor Spheroid-Based Migration Assays for Evaluation of Therapeutic Agents. In: Moll J, Colombo R, editors. Target Identification and Validation in Drug Discovery. Totowa, NJ: Humana Press; 2013. p. 253–66. (Methods in Molecular Biology; vol. 986).

78. Conceição A. Understanding the impact of alterations in the expression of LAMA2 in melanoma [Master thesis]. [Lisbon]: NOVA university Lisbon; 2023.

79. Mazurkiewicz J, Simiczyjew A, Dratkiewicz E, Pietraszek-Gremplewicz K, Majkowski M, Kot M, et al. Melanoma cells with diverse invasive potential differentially induce the activation of normal human fibroblasts. Cell Commun Signal. 2022 Dec;20(1):63.

80. Alam Y, Borowicz P, W. Vetter S, Leclerc E. Using Tumor-Like Spheroids to Study the Effect of Anti-Cancer Drugs *In Vitro*. In: Basu S, Ranjan A, Sur S, editors. Biochemistry. IntechOpen; 2024.

81. Marzagalli M, Moretti RM, Messi E, Marelli MM, Fontana F, Anastasia A, et al. Targeting melanoma stem cells with the Vitamin E derivative δ-tocotrienol. Sci Rep. 2018 Jan 12;8(1):587.

82. Gomes LR, Vessoni AT, Menck CFM. Three-dimensional microenvironment confers enhanced sensitivity to doxorubicin by reducing p53-dependent induction of autophagy. Oncogene. 2015 Oct 16;34(42):5329–40.

83. He J, Liang X, Luo F, Chen X, Xu X, Wang F, et al. P53 Is Involved in a Three-Dimensional Architecture-Mediated Decrease in Chemosensitivity in Colon Cancer. J Cancer. 2016;7(8):900–9.

84. Ravi M, Paramesh V, Kaviya SR, Anuradha E, Solomon FDP. 3D Cell Culture Systems: Advantages and Applications. J Cell Physiol. 2015 Jan;230(1):16–26.

85. Barraza-Flores P, Bates CR, Oliveira-Santos A, Burkin DJ. Laminin and Integrin in LAMA2-Related Congenital Muscular Dystrophy: From Disease to Therapeutics. Front Mol Neurosci. 2020 Feb 11;13:1.

86. Ma N, Xu E, Luo Q, Song G. Rac1: A Regulator of Cell Migration and a Potential Target for Cancer Therapy. Molecules. 2023 Mar 27;28(7):2976.

87. Feng L, Pan R, Ning K, Sun W, Chen Y, Xie Y, et al. The impact of 3D tumor spheroid maturity on cell migration and invasion dynamics. Biochem Eng J. 2025 Jan;213:109567.

88. Guan X, Guan X, Dong C, Jiao Z. Rho GTPases and related signaling complexes in cell migration and invasion. Exp Cell Res. 2020 Mar;388(1):111824.

89. Chang F, Lemmon CA, Park D, Romer LH. FAK Potentiates Rac1 Activation and Localization to Matrix Adhesion Sites: A Role for βPIX. Parent C, editor. Mol Biol Cell. 2007 Jan;18(1):253–64.

90. Fortunato IC, Brückner DB, Grosser S, Rossetti L, Bosch-Padrós M, Trebicka J, et al. Single cell migration along and against confined haptotactic gradients. Cell Biology; 2024.

91. Suh HN, Han HJ. Laminin regulates mouse embryonic stem cell migration: involvement of Epac1/Rap1 and Rac1/cdc42. Am J Physiol-Cell Physiol. 2010 May;298(5):C1159–69.

92. Yu WM, Chen ZL, North AJ, Strickland S. Laminin is required for Schwann cell morphogenesis. J Cell Sci. 2009 Apr 1;122(7):929–36.

93. Gadea G, De Toledo M, Anguille C, Roux P. Loss of p53 promotes RhoA–ROCK-dependent cell migration and invasion in 3D matrices. J Cell Biol. 2007 July 2;178(1):23–30.

94. Gadea G. Regulation of Cdc42-mediated morphological effects: a novel function for p53. EMBO J. 2002 May 15;21(10):2373–82.

95. Guo F, Gao Y, Wang L, Zheng Y. p19Arf-p53 Tumor Suppressor Pathway Regulates Cell Motility by Suppression of Phosphoinositide 3-Kinase and Rac1 GTPase Activities. J Biol Chem. 2003 Apr;278(16):14414–9.

96. Bosco EE, Ni W, Wang L, Guo F, Johnson JF, Zheng Y. Rac1 targeting suppresses p53 deficiency–mediated lymphomagenesis. Blood. 2010 Apr 22;115(16):3320–8.

97. Yue X, Zhang C, Zhao Y, Liu J, Lin AW, Tan VM, et al. Gain-of-function mutant p53 activates small GTPase Rac1 through SUMOylation to promote tumor progression. Genes Dev. 2017 Aug 15;31(16):1641–54.

98. Zhang C, Liu J, Zhao Y, Yue X, Zhu Y, Wang X, et al. Glutaminase 2 is a novel negative regulator of small GTPase Rac1 and mediates p53 function in suppressing metastasis. eLife. 2016 Jan 11;5:e10727.

99. Zhu J, Mogilner A. Comparison of cell migration mechanical strategies in three-dimensional matrices: a computational study. Interface Focus. 2016 Oct 6;6(5):20160040.

100. Caley MP, Martins VLC, O'Toole EA. Metalloproteinases and Wound Healing. Adv Wound Care. 2015 Apr;4(4):225–34.

6. Annex

Supplementary Table 1: Antibodies used in western blot and immunofluorescence.

Antibody	Raised in	Primary vs Secondary	Dilution	Catalog number	Brand
p-p53	rabbit	primary	1/1000	#9284	Cell Signaling Technology
p53	mouse	primary	1/1000	2524	Cell Signaling Technology
GAPDH	rabbit	primary	1/1000	2118S	Cell Signaling Technology
Caspase-3 (cleaved)	rabbit	primary	1/1000	9661	Cell Signaling Technology
Ki67	rabbit	primary	pre-diluted		Roche (Ventana)
Anti-rabbit IgG-HRP	Donkey	Secondary	1/5000	NA934	GE Healthcare
Anti-Mouse-HRP	Sheep	Secondary	1/5000	NA931	GE Healthcare

Supplementary Table 2: Primers used for gene expression analysis by qRT-PCR .

Gene	Primer	Sequence	Amplicon size
Actin	Forward	GAGCACAGAGCCTCGCCTT	
Actin	Reverse	TCATCATCCATGGTGAGCTGG	70
TIMP1	Forward	GCGGATACTTCCACAGGTCC	
TIMP1	Reverse	AAACAGGGAAACACTGTGCAT	190
RAC1	Forward	ACAGATTACGCCCCCTATCCT	
RAC1	Reverse	ATGATGCAGGACTCACAAGG	75

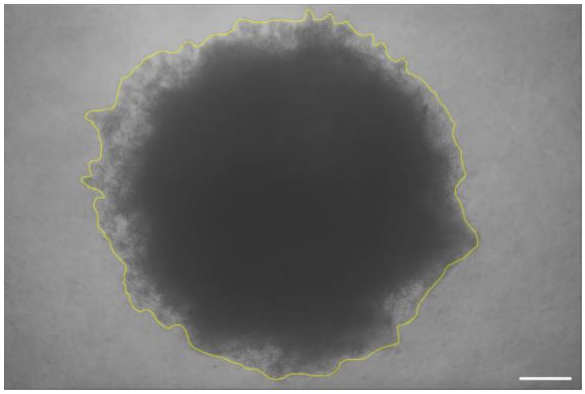

Supplementary Figure 1: Representative figure of the overlay to measure the spheroids area. Scale bar: 250 µm.

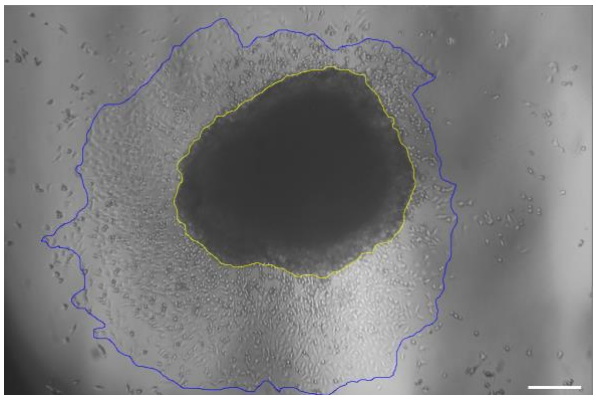

Supplementary Figure 2: Representative figure of the overlay draw, in core and the total area for measure the migration area. Scale bar: 250 μm.